MOX-Report No. 09/2019

Unified analysis of Discontinuous Galerkin approximations of flows in fractured porous media on polygonal and polyhedral grids

Antonietti, P.F.; Facciola', C.; Verani, M.

MOX, Dipartimento di Matematica
Politecnico di Milano, Via Bonardi 9 - 20133 Milano (Italy)

mox-dmat@polimi.it http://mox.polimi.it

Unified analysis of Discontinuous Galerkin approximations of flows in fractured porous media on polygonal and polyhedral grids *

Paola F. Antonietti[#], Chiara Facciolà[#] and Marco Verani[#]

March 22, 2019

[#] MOX- Laboratory for Modeling and Scientific Computing
Dipartimento di Matematica
Politecnico di Milano
Piazza Leonardo da Vinci 32, 20133 Milano, Italy
paola.antonietti@polimi.it, chiara.facciola@polimi.it, marco.verani@polimi.it

Abstract

We propose a unified formulation based on discontinuous Galerkin methods on polygonal/polyhedral grids for the simulation of flows in fractured porous media. We adopt a model for single-phase flows where the fracture is modeled as a $(d-1)$ - dimensional interface in a d - dimensional bulk domain, and model the flow in the porous medium and in the fracture by means of the Darcy's law. The two problems are then coupled through physically consistent conditions. We focus on the numerical approximation of the coupled bulk-fracture problem and present and analyze, in the unified setting of [20], all the possible combinations of primal-primal, mixed-primal, primal-mixed and mixed-mixed formulations for the bulk and fracture problems, respectively. For all the possible combinations, we prove their well-posedness and derive a priori hp-version error estimates in a suitable (mesh-dependent) energy norm. Finally, several numerical experiments assess the theoretical error estimates and verify the practical performance of the proposed schemes.

Introduction

Many Geophysical and Engineering applications, including, for example, fluid-structure interaction, crack and wave propagation problems, and flow in fractured porous media, are characterized by a strong complexity of the physical domain, possibly involving thousands of fault/fractures, heterogeneous media, moving geometries/interfaces and complex topographies. Whenever classical Finite-Element-based approaches are employed to discretize the underlying differential model, the process of mesh generation can be the bottleneck of the

*Paola F. Antonietti and Chiara Facciolà have been partially supported by SIR Starting grant n. RBSI14VT0S "PolyPDEs: Non-conforming polyhedral finite element methods for the approximation of partial differential equations" funded by MIUR. All the authors have been partially supported by INdAM-GNCS.

whole simulation, as classical finite elements only support computational grids composed by tetrahedral/hexahedral/prismatic elements. To overcome this limitation, in the last decade a wide strand of literature focused on the design of numerical methods that support computational meshes composed of general polygonal and polyhedral (polytopic, for short) elements. In the conforming setting, we mention for example the Composite Finite Element Method [59, 58], the Mimetic Finite Difference method [60, 33, 31, 32, 28, 10], the Polygonal Finite Element Method [67], the Extended Finite Element Method [68, 55], the Virtual Element Method [25, 26, 27, 7, 8] and the Hybrid High-Order method [50, 48, 49, 51]. In the setting of non-conforming/discontinuos polygonal methods, we mention, for example, Hybridizable Discontinuous Galerkin methods [42, 43, 44, 45], Composite Discontinuous Finite Element methods [11, 12], non-conforming VEM [16, 21, 39], Gradient Schemes [52] and the polytopic Discontinuous Galerkin method [5, 23, 24, 22, 11, 12, 38, 36, 37, 14, 6, 17, 4, 18, 15].

Within this framework, we focus our attention on the problem of modelling the flow in a fractured porous medium, which is fundamental in many energy or environmental engineering applications, such as tracing oil migration, isolation of radioactive waste, groundwater contamination, etc. Fractures are regions of the porous medium that are typically characterized both by a different porous structure and by a very small width. The first feature implies that fractures have a very strong impact on the flow, since they can possibly act as barriers or as preferential paths for the fluid. The second feature entails the need for a very large number of elements for the discretization of the fracture layer and, consequently, a high computational cost. For this reason, one popular modelling choice consists in a reduction strategy, so that fractures are treated as $(d-1)$-dimensional interfaces between d-dimensional porous matrices, $d = 2, 3$. In particular, we refer to the model for single-phase flow developed in [2, 1, 62, 56]. Here, the flow in the porous medium (bulk) is assumed to be governed by Darcy's law and a suitable reduced version of the law is formulated on the surface modelling the single fracture. The two problems are then coupled through physically consistent conditions to account for the exchange of fluid between them. We remark that this model is able to handle both fractures with low and large permeability. Moreover, its extension to the case of two-phase flows has been addressed in [57, 61], while the case of a totally immersed fracture has been considered e.g. in [3].

Even if the use of this kind of dimensionally reduced models avoids the need for extremely refined grids inside the fracture domains, in realistic cases, the construction of a computational grid aligned with the fractures is still a major issue. For example, a fractured oil reservoir can be cut by several thousands of fractures, which often intersect, create small angles or are nearly coincident [54]. In line with the previous discussion, in order to avoid the limitations imposed by standard finite element methods, various numerical methods supporting polytopic elements have been employed in the literature for the approximation of the coupled bulk-fracture problem. For example, in [10, 54] a mixed approximation based on the use of Mimetic Finite Difference method has been explored; in [29, 30] a framework for treating flows in Discrete Fracture Networks based on the Virtual Element Method has been introduced, and in [41] the Hybrid High-Order method has been employed. We also mention that an alternative strategy consists in the use of non-conforming discretizations, where fractures are allowed to arbitrarily cut the bulk grid, which can then be chosen fairly regular. In particular, we refer to [47, 57, 53], where an approximation employing eXtended Finite Element Method (XFEM) has been proposed and to the recent work [34], where the use of

the cut Finite Element Method (CUTFEM) has been explored.

Recently in [9], in the setting of conforming discretizations, we developed a numerical approximation of the coupled bulk-fracture model based on polytopic Discountinuous Galerkin (PolyDG) methods. In particular, the intrinsic "discontinuous" nature of DG methods allows very general polytopic elements because of the freedom in representing the underlying (local) polynomial space. Indeed the degrees of freedom are not "attached" to any geometric quantity, (vertexes, edges, etcc), so that mesh elements with edges/faces that may be in arbitrary number and whose measure may be arbitrarily small compared to the diameter of the corresponding element are naturally supported with a solid theoretical background. This approach is then very well suited to tame the geometrical complexity featured by most of applications in the computational geoscience field. Moreover, since the interface conditions between the bulk and fracture problem can be naturally formulated using jump and average operators, the coupling of the two problems can be naturally embedded in the variational formulation.

The goal of this paper is to extend the results obtained in [9], where the proposed discretization based on PolyDG was in a primal-primal setting. Here, we design and analyze, in the *unified* framework of [20] based on the *flux-formulation*, all the possible combinations of primal-primal, mixed-primal, primal-mixed and mixed-mixed formulations for the bulk and fracture problems, respectively. In particular, the primal discretizations are obtained using the Symmetric Interior Penalty discontinuous Galerkin method [70, 19], whereas the mixed discretizations are based on employing the local DG (LDG) method of [46]. Moreover, the coupling conditions between bulk and fracture are imposed through a suitable definition of the numerical fluxes on the fracture faces. Such an abstract setting allows to analyse theoretically at the same time all the possible formulations.

We perform a unified analysis of all the derived combinations of DG discretizations for the bulk-fracture problem. We prove their well-posedness and derive a priori *hp*-version error estimates in a suitable (mesh-dependent) energy norm. Finally, we present numerical experiments assessing the validity of the theoretical error estimates and testing and comparing the practical performance of the proposed formulations.

The rest of the paper is organized as follows. In Section 1 we introduce the model problem; its weak formulation is discussed in Section 2. The discretization based on employing PolyDG methods is presented, in the unified setting of [20], in Section 3. In Section 4, we address the problem of stability and prove that all formulations, namely primal-primal (PP), mixed-primal (MP), primal-mixed (PM) and mixed-mixed (MM) are well-posed. The corresponding error analysis is presented in Section 5. Several numerical tests, focusing, for the sake of brevity, on the mixed-primal (MP) case, are presented in Section 6 to confirm the theoretical bounds. Moreover, we assess the capability of the method of handling more complicated geometries, presenting some test cases featuring networks of partially immersed fractures.

1 Model problem

For simplicity, we consider the case where the porous medium is cut by a single, non immersed fracture. The extension to the case of a network of disjoint fractures can be treated analogously. The case where the fracture is partially or totally immersed in the

domain is more complex to analyze, and we refer to [3, 54] for its discussion. Nevertheless, the capability of our method to deal with networks of partially immersed fractures will be explored via numerical experiments in Section 6.3 in the mixed-primal setting (MP). Finally, the case of a network of interecting fractures will be the object of a future work and we refer to [9] for preliminary numerical results (in the primal-primal setting) showing that our method is able to handle also such cases.

The porous matrix is represented by the domain $\Omega \subset \mathbb{R}^d$, $d = 2, 3$, which we assume to be open, bounded, convex and polygonal/polyhedral. Moreover, following the strategy of [62], we suppose that the fracture may be described by the $(d-1)$-dimensional $\mathcal{C}^\infty$ manifold (with no curvature) $\Gamma \subset \mathbb{R}^{d-1}$, $d = 2, 3$. This approach is justified by the fact that the thickness of the fracture domain is typically some orders of magnitude smaller than the size of the domain. Since we are assuming that Γ is not immersed, it separates Ω into two connected disjoint subdomains, $\Omega \setminus \Gamma = \Omega_1 \cup \Omega_2$ with $\Omega_1 \cap \Omega_2 = \emptyset$. We decompose the boundary of Ω into two disjoint subsets $\partial\Omega_D$ and $\partial\Omega_N$, *i.e.*, $\partial\Omega = \partial\Omega_D \cup \partial\Omega_N$, with $\partial\Omega_D \cap \partial\Omega_N = \emptyset$, and we define $\partial\Omega_{D,i} = \partial\Omega_D \cap \partial\Omega_i$ and $\partial\Omega_{N,i} = \partial\Omega_N \cap \partial\Omega_i$, for $i = 1, 2$. Finally, we denote by $\mathbf{n}_i$, $i = 1, 2$ the unit normal vector to Γ pointing outwards from Ω_i and, for a (regular enough) scalar-valued function q and a (regular enough) vector-valued function $\mathbf{v}$, we define the classical *jump* and *average* operators across the fracture Γ as

$$\begin{aligned} \{q\} &= \frac{1}{2}(q_1 + q_2) \qquad & [\![q]\!] &= q_1\mathbf{n}_1 + q_2\mathbf{n}_2, \\ \{\mathbf{v}\} &= \frac{1}{2}(\mathbf{v}_1 + \mathbf{v}_2) \qquad & [\![\mathbf{v}]\!] &= \mathbf{v}_1 \cdot \mathbf{n}_1 + \mathbf{v}_2 \cdot \mathbf{n}_2, \end{aligned} \tag{1}$$

where the subscript $i = 1, 2$ denotes the restriction to the subdomain Ω_i. Note that, since we are assuming that the fracture has no curvature, it holds $\mathbf{n}_1 = -\mathbf{n}_2$. In Figure 1 we report an example of domain cut by a single fracture.

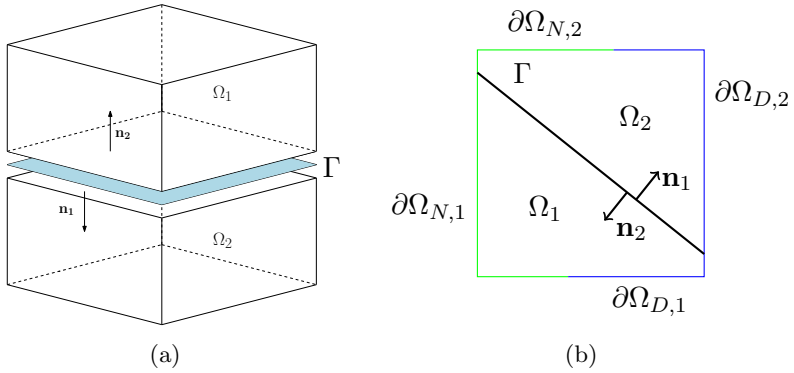

Figure 1: The subdomains Ω_1 and Ω_2 separated by the fracture Γ considered as an interface, for $d = 3$ (left) and $d = 2$ (right).

We can now introduce the governing equations for our model. In the bulk, we suppose that the flow is governed by Darcy's law. The motion of an incompressible fluid in each

domain Ω_i, $i = 1, 2$, with pressure p_i and velocity $\mathbf{u}_i$ may then be described by:

$$\begin{cases} \mathbf{u}_i = \boldsymbol{\nu}_i \nabla p_i & \text{in } \Omega_i, \\ -\nabla \cdot \mathbf{u}_i = f_i & \text{in } \Omega_i, \\ p_i = g_{D,i} & \text{on } \partial\Omega_{D,i}, \\ \mathbf{u}_i \cdot \mathbf{n}_i = 0 & \text{on } \partial\Omega_{N,i}, \end{cases} \tag{2}$$

where $f \in L^2(\Omega)$ represents a source term, $g_D \in H^{1/2}(\partial\Omega_D)$ is the Dirichlet boundary datum and $\boldsymbol{\nu} = \boldsymbol{\nu}(x) \in \mathbb{R}^{d\times d}$ is the bulk permeability tensor, which we assume to be symmetric, positive definite, uniformly bounded from below and above and with entries that are bounded, piecewise continuous real-valued functions.

On the manifold Γ representing the fracture, we formulate a reduced version of Darcy's law in the tangential direction (we refer to [62] for a rigorous derivation of the model). To this aim we assume that the fracture permeability tensor $\boldsymbol{\nu}_\Gamma$, has a block-diagonal structure of the form

$$\boldsymbol{\nu}_\Gamma = \begin{bmatrix} \nu_\Gamma^n & 0 \\ 0 & \boldsymbol{\nu}_\Gamma^\tau \end{bmatrix}, \tag{3}$$

when written in its normal and tangential components. Here, $\boldsymbol{\nu}_\Gamma^\tau \in \mathbb{R}^{(d-1)\times(d-1)}$ is a positive definite, uniformly bounded tensor (it reduces to a positive number for $d = 2$). Moreover, we assume that $\boldsymbol{\nu}_\Gamma$ satisfies the same regularity assumptions as those satisfied by the bulk permeability $\boldsymbol{\nu}$. Setting $\partial\Gamma = \Gamma \cap \partial\Omega$, $\partial\Gamma = \partial\Gamma_D \cup \partial\Gamma_N$, introducing the fracture thickness $\ell_\Gamma > 0$ and denoting by p_Γ and $\mathbf{u}_\Gamma$ the fracture pressure and velocity, the governing equations for the fracture flow are

$$\begin{cases} \mathbf{u}_\Gamma = \boldsymbol{\nu}_\Gamma^\tau \ell_\Gamma \nabla_\tau p_\Gamma & \text{in } \Gamma, \\ -\nabla_\tau \cdot \mathbf{u}_\Gamma = f_\Gamma - [\![\mathbf{u}]\!] & \text{in } \Gamma, \\ p_\Gamma = g_\Gamma & \text{on } \partial\Gamma_D, \\ \mathbf{u}_\Gamma \cdot \boldsymbol{\tau} = 0 & \text{on } \partial\Gamma_N, \end{cases} \tag{4}$$

where $f_\Gamma \in L^2(\Gamma)$, $g_\Gamma \in H^{1/2}(\partial\Gamma)$, $\boldsymbol{\tau}$ is vector in the tangent plane of Γ normal to $\partial\Gamma$ and ∇_τ and $\nabla_\tau\cdot$ denote the tangential gradient and divergence operators, respectively.

Finally, following [62], we close the model providing the interface conditions to couple problems (2) and (4) along their interface. Given a positive real number $\xi \neq \frac{1}{2}$ that will be chosen later on, the coupling conditions read as follows

$$-\{\mathbf{u}\} = \beta_\Gamma [\![p]\!] \qquad \text{on } \Gamma, \tag{5a}$$

$$-[\![\mathbf{u}]\!] = \alpha_\Gamma (\{p\} - p_\Gamma) \qquad \text{on } \Gamma, \tag{5b}$$

where $\beta_\Gamma = \frac{1}{2\eta_\Gamma}$ and $\alpha_\Gamma = \frac{2}{\eta_\Gamma(2\xi-1)}$ and $\eta_\Gamma = \frac{\ell_\Gamma}{\nu_\Gamma^n}$, ν_Γ^n being the normal component of the fracture permeability tensor, see (3).

In conclusion, the coupled bulk-fracture model problem is the following:

$$\begin{cases} \mathbf{u}_i = \boldsymbol{\nu}_i \nabla p_i & \text{in } \Omega_i, \\ -\nabla \cdot \mathbf{u}_i = f_i & \text{in } \Omega_i, \\ p_i = g_{D,i} & \text{on } \gamma_{D,i}, \\ \mathbf{u}_i \cdot \mathbf{n}_i = 0 & \text{on } \gamma_{N,i} \\ \mathbf{u}_\Gamma = \boldsymbol{\nu}_\Gamma^\tau \ell_\Gamma \nabla_\tau p_\Gamma & \text{in } \Gamma, \\ -\nabla_\tau \cdot \mathbf{u}_\Gamma = f_\Gamma - [\![\mathbf{u}]\!] & \text{in } \Gamma, \\ p_\Gamma = g_\Gamma & \text{on } \partial\Gamma_D, \\ \mathbf{u}_\Gamma \cdot \boldsymbol{\tau} = 0 & \text{on } \partial\Gamma_N, \\ -\{\mathbf{u}\} = \beta_\Gamma [\![p]\!] & \text{on } \Gamma, \\ -[\![\mathbf{u}]\!] = \alpha_\Gamma(\{p\} - p_\Gamma) & \text{on } \Gamma. \end{cases} \tag{6}$$

2 Weak formulation

In this section we introduce the weak formulation of our model problem (6) and prove its well-posedness. We start with the introduction of the functional setting.

2.1 Functional setting

We will employ the following notation. For an open, bounded domain $D \subset \mathbb{R}^d$, $d = 2, 3$, we denote by $H^s(D)$ the standard Sobolev space of order s, for a real number $s \geq 0$. For $s = 0$, we write $L^2(D)$ in place of $H^0(D)$. The usual norm on $H^s(D)$ is denoted by $||\cdot||_{s,D}$ and the usual seminorm by $|\cdot|_{s,D}$. We also introduce the standard space $H_{div}(D) = \{\mathbf{v} : D \to \mathbb{R}^d : ||\mathbf{v}||_{0,D} + ||\nabla \cdot \mathbf{v}||_{0,D} < \infty\}$. Given a decomposition of the domain into elements $\mathcal{T}_h$, we will denote by $H^s(\mathcal{T}_h)$ the standard *broken* Sobolev space, equipped with the broken norm $||\cdot||_{s,\mathcal{T}_h}$. Furthermore, we will denote by $\mathbb{P}_k(D)$ the space of polynomials of *total* degree less than or equal to $k \geq 1$ on D. The symbol $\lesssim$ (and $\gtrsim$) will signify that the inequalities hold up to multiplicative constants which are independent of the discretization parameters, but might depend on the physical parameters.

Next, we introduce the functional spaces for our weak formulation. For the bulk pressure and velocity, we introduce the spaces $M^b = L^2(\Omega)$ and $\mathbf{V}^b = \{\mathbf{v} \in H_{div}(\Omega) : [\![\mathbf{v}]\!]|_\Gamma \in L^2(\Gamma), \{\mathbf{v}\}|_\Gamma \in [L^2(\Gamma)]^d, \mathbf{v} \cdot \mathbf{n}|_{\partial\Omega_N} = 0\}$, and equip the space $\mathbf{V}^b$ with the norm $||\mathbf{v}||^2_{\mathbf{V}^b} = ||\mathbf{v}||^2_{0,\Omega} + ||\nabla \cdot \mathbf{v}||^2_{0,\Omega} + ||[\![\mathbf{v}]\!]||^2_{0,\Gamma} + ||\{\mathbf{v}\}||^2_{0,\Gamma}$.

Similarly, for the fracture pressure and velocity we define the spaces $M^\Gamma = L^2(\Gamma)$ and $\mathbf{V}^\Gamma = \{\mathbf{v}_\Gamma \in H_{div,\tau}(\Gamma) : \mathbf{v}_\Gamma \cdot \boldsymbol{\tau}|_{\partial\Gamma} = 0\}$. The norm on $\mathbf{V}^\Gamma$ is given by $||\mathbf{v}_\Gamma||^2_{\mathbf{V}^\Gamma} = ||\mathbf{v}_\Gamma||^2_{0,\Gamma} + ||\nabla_\tau \cdot \mathbf{v}_\Gamma||^2_{0,\Gamma}$. Finally, we define the global spaces for the pressure and the velocity as $M = M^b \times M^\Gamma$ and $\mathbf{W} = \mathbf{V}^b \times \mathbf{V}^\Gamma$, equipped with the canonical norms for product spaces. In order to deal with non-homogeneous boundary conditions, we also introduce the affine spaces $V_g^b = \mathcal{L}_g + \mathbf{V}^b$ and $V_g^\Gamma = \mathcal{L}_{g_\Gamma} + \mathbf{V}^\Gamma$, where $\mathcal{L}_g \in H_{div}(\Omega)$ and $\mathcal{L}_{g_\Gamma} \in H_{div,\tau}(\Gamma)$ are liftings of the boundary data g and g_Γ, respectively. We can then define the global space $\mathbf{W}_g = \mathbf{V}_g^b \times \mathbf{V}_g^\Gamma$.

2.2 Weak problem

We can now formulate problem (6) in weak form as follows: Find $(\mathbf{u}, \mathbf{u}_\Gamma) \in \mathbf{W}_g$ and $(p, p_\Gamma) \in M$ such that

$$\begin{cases} A((\mathbf{u}, \mathbf{u}_\Gamma), (\mathbf{v}, \mathbf{v}_\Gamma)) + B((\mathbf{v}, \mathbf{v}_\Gamma), (p, p_\Gamma)) = F^{\mathbf{u}}(\mathbf{v}, \mathbf{v}_\Gamma) \\ -B((\mathbf{u}, \mathbf{u}_\Gamma), (q, q_\Gamma)) = F^{p}(q, q_\Gamma) \end{cases} \tag{7}$$

where the bilinear form $A(\cdot,\cdot) : \mathbf{W}_q \times \mathbf{W}_g \to \mathbb{R}$ is defined as $A((\mathbf{u}, \mathbf{u}_\Gamma), (\mathbf{v}, \mathbf{v}_\Gamma)) = a(\mathbf{u}, \mathbf{v}) + a_\Gamma(\mathbf{u}_\Gamma, \mathbf{v}_\Gamma)$ with

$$\begin{aligned} a(\mathbf{u}, \mathbf{v}) &= \int_\Omega \boldsymbol{\nu}^{-1}\mathbf{u} \cdot \mathbf{v} + \int_\Gamma \frac{1}{\alpha_\Gamma} [\![\mathbf{u}]\!][\![\mathbf{v}]\!] + \int_\Gamma \frac{1}{\beta_\Gamma} \{\mathbf{u}\} \cdot \{\mathbf{v}\}, \\ a_\Gamma(\mathbf{u}_\Gamma, \mathbf{v}_\Gamma) &= \int_\Gamma (\boldsymbol{\nu}_\Gamma^\tau \ell_\Gamma)^{-1} \mathbf{u}_\Gamma \cdot \mathbf{v}_\Gamma, \end{aligned}$$

and the bilinear form $B(\cdot,\cdot) : \mathbf{W}_g \times M \to \mathbb{R}$ is defined as $B((\mathbf{v}, \mathbf{v}_\Gamma), (q, q_\Gamma)) = b(\mathbf{v}, q) + b_\Gamma(\mathbf{v}_\Gamma, q_\Gamma) + d(\mathbf{v}, q_\Gamma)$, with

$$b(\mathbf{v}, q) = \int_\Omega \nabla \cdot \mathbf{v}\, q, \qquad b_\Gamma(\mathbf{v}_\Gamma, q_\Gamma) = \int_\Gamma \nabla_\tau \cdot \mathbf{v}_\Gamma\, q_\Gamma, \qquad d(\mathbf{v}, q_\Gamma) = -\int_\Gamma [\![\mathbf{v}]\!] q_\Gamma.$$

Finally the linear operators $F^{\mathbf{u}}(\cdot) : \mathbf{W}_g \to \mathbb{R}$ and $F^{p}(\cdot) : M \to \mathbb{R}$ are defined as

$$F^{\mathbf{u}}(\mathbf{v}, \mathbf{v}_\Gamma) = \int_{\partial\Omega} g\mathbf{v} \cdot \mathbf{n} + \int_{\partial\Gamma} g_\Gamma \mathbf{v}_\Gamma \cdot \boldsymbol{\tau}, \qquad F^{p}(q, q_\Gamma) = \int_\Omega fq + \int_\Gamma f_\Gamma q_\Gamma.$$

Next, we prove that formulation (7) is well-posed. For the sake of simplicity, we will assume that homogeneous Dirichlet boundary conditions are imposed for both the bulk and fracture problems, i.e., $g_{D,i} = 0$, $i = 1; 2$, and $g_\Gamma = 0$ and that the domain and fracture are smooth enough. The extension to the general non-homogeneous case is straightforward. Note that the existence and uniqueness of the problem can be proven only under the condition that the parameter $\xi > 1/2$.

Theorem 2.1. *Suppose that $\xi > 1/2$. Then problem (7) admits a unique solution.*

Proof. For the proof we follow the technique of [62]. First, we define the subspace of $\mathbf{W}$, $\widehat{\mathbf{W}} = \{(\mathbf{v}, \mathbf{v}_\Gamma) \in \mathbf{W} : B((\mathbf{v}, \mathbf{v}_\Gamma), (q, q_\Gamma)) = 0 \ \forall (q, q_\Gamma) \in M\}$. To show existence and uniqueness of the solution of (7), we only need to show that $A(\cdot,\cdot)$ is $\widehat{\mathbf{W}}$-elliptic and that $B(\cdot,\cdot)$ satisfies the inf-sup condition, that is

$$\inf_{(\mathbf{v}, \mathbf{v}_\Gamma) \in \widehat{\mathbf{W}}} \frac{A((\mathbf{v}, \mathbf{v}_\Gamma), (\mathbf{v}, \mathbf{v}_\Gamma))}{||(\mathbf{v}, \mathbf{v}_\Gamma)||^2_{\mathbf{W}}} \gtrsim 1, \qquad \inf_{(q, q_\Gamma) \in M} \sup_{(\mathbf{v}, \mathbf{v}_\Gamma) \in \mathbf{W}} \frac{B((\mathbf{v}, \mathbf{v}_\Gamma), (q, q_\Gamma))}{||(q, q_\Gamma)||_M ||(\mathbf{v}, \mathbf{v}_\Gamma)||_{\mathbf{W}}} \gtrsim 1.$$

First, we prove that $A(\cdot,\cdot)$ is $\widehat{\mathbf{W}}$-elliptic. Since for elements in $(\mathbf{v}, \mathbf{v}_\Gamma) \in \widehat{\mathbf{W}}$ we have $\nabla \cdot \mathbf{v} = 0$ in $L^2(\Omega)$ and $\nabla_\tau \cdot \mathbf{v}_\Gamma = [\![\mathbf{v}]\!]|_\Gamma$ in $L^2(\Gamma)$, the norm $||(\mathbf{v}, \mathbf{v}_\Gamma)||_{\mathbf{W}}$ is equivalent to $||\mathbf{v}||^2_{0,\Omega} + ||\mathbf{v}_\Gamma||^2_{0,\Gamma} + ||[\![v]\!]||^2_{0,\Gamma} + ||\{\mathbf{v}\}||^2_{0,\Gamma}$. Owing to the regularity properties of the permeability tensors $\boldsymbol{\nu}$ and $\boldsymbol{\nu}_\Gamma$, this implies that

$$A((\mathbf{v}, \mathbf{v}_\Gamma), (\mathbf{v}, \mathbf{v}_\Gamma)) \gtrsim ||(\mathbf{v}, \mathbf{v}_\Gamma)||^2_{\mathbf{W}}.$$

Note that the hidden constant also depends on the parameter α_Γ, and that we need to assume $\alpha_\Gamma > 0$, or, equivalently, $\xi > 1/2$, for the inequality to hold true.

To show that B satisfies the inf-sup condition, given $(q, q_\Gamma) \in M$, we construct, exploiting the adjoint problem, $(\mathbf{v}, \mathbf{v}_\Gamma) \in \mathbf{W}$ such that $B((\mathbf{v}, \mathbf{v}_\Gamma), (q, q_\Gamma)) = ||(q, q_\Gamma)||_M^2$ and $||(\mathbf{v}, \mathbf{v}_\Gamma)||_{\mathbf{W}} \lesssim ||(q, q_\Gamma)||_M$. Given $(q, q_\Gamma) \in M$, let (ϕ, ϕ_Γ) be the solution of

$$\begin{cases} -\Delta\phi = q, & \text{on } \Omega \\ \phi = 0, & \text{on } \partial\Omega \end{cases} \qquad \text{and} \qquad \begin{cases} -\Delta_\tau\phi_\Gamma = q_\Gamma, & \text{on } \Gamma \\ \phi_\Gamma = 0, & \text{on } \partial\Gamma. \end{cases}$$

If we set $\mathbf{v} = (\mathbf{v}_1, \mathbf{v}_2)$ with $\mathbf{v}_i = -\nabla\phi|_{\Omega_i}$, $i = 1, 2$, and $\mathbf{v}_\Gamma = -\nabla_\tau\phi_\Gamma$, we obtain $\nabla \cdot \mathbf{v} = q$, $\nabla_\tau \cdot \mathbf{v}_\Gamma = q_\Gamma$ and $[\![\mathbf{v}]\!]|_\Gamma = 0$, since $\mathbf{v} \in H^1(\Omega)$. This implies that $(\mathbf{v}, \mathbf{v}_\Gamma) \in \mathbf{W}$ and $B((\mathbf{v}, \mathbf{v}_\Gamma), (q, q_\Gamma)) = ||q||_{0,\Omega}^2 + ||q_\Gamma||_{0,\Gamma}^2 = ||(q, q_\Gamma)||_M^2$. Finally, from elliptic regularity, we have $||(\mathbf{v}, \mathbf{v}_\Gamma)||_{\mathbf{W}}^2 = ||\nabla\phi||_{0,\Omega}^2 + ||\nabla_\tau\phi_\Gamma||_{0,\Gamma}^2 + ||q||_{0,\Omega}^2 + ||q_\Gamma||_{0,\Gamma}^2 + ||\{\nabla\phi\}||_{0,\Gamma}^2 \lesssim ||q||_{0,\Omega}^2 + ||q_\Gamma||_{0,\Gamma}^2$, and this concludes the proof.

□

3 Numerical dicretization based on PolyDG methods

In this section we present a family of discrete formulations for the coupled bulk-fracture problem (7), which are based on Discontinuous Galerkin methods on polytopic grids. In particular, since we can choose to discretize the problem in the bulk and the one in the fracture either in their mixed or in their primal form, we derive four formulations that embrace all the possible combinations of primal-primal, mixed-primal, primal-mixed and mixed-mixed discretizations. The mixed discretizations will be based on the Local Discontinuous Galerkin method (LDG) [46, 40, 64], while the primal discretizations on the Symmetric Interior Penalty method (SIPDG) [19, 70], all supporting polytopic grids [38, 36, 6, 37]. The derivation of our discrete formulations will be carried out following the same strategy as in [20], so that it will be based on the introduction of the *numerical fluxes*, which approximate the trace of the solutions on the boundary of each mesh element. In particular, the imposition of the coupling conditions (5a)-(5b) will be achieved through a proper definition of the numerical fluxes on the faces belonging to the fracture.

First, we introduce the notation related to the discretization of the domains by means of polytopic meshes. For the problem in the bulk, we consider a family of meshes $\mathcal{T}_h$ made of disjoint open *polygonal/polyhedral* elements. Following [38, 36, 6], we introduce the concept of mesh *interface*, defined as the intersection of the $(d-1)$-dimensional facets of two neighbouring elements. We need now to distinguish between the case when $d = 3$ and $d = 2$:

- when $d = 3$, each interface consists of a general polygon, which we assume may be decomposed into a set of co-planar triangles. We assume that a sub-triangulation of each interface is provided and we denote the set of all these triangles by $\mathcal{F}_h$. We then use the terminology *face* to refer to one of the triangular elements in $\mathcal{F}_h$;

- when $d = 2$, each interface simply consists of a line segment, so that the concepts of face and interface are in this case coincident. We still denote by $\mathcal{F}_h$ the set of all faces.

Note that $\mathcal{F}_h$ is always defined as a set of $(d-1)$-dimensional simplices (triangles or line segments). As in [38, 36, 6], no limitation on either the number of faces of each polygon

$E \in \mathcal{T}_h$ or on the relative size of the faces compared to the diameter of the element is imposed.
We consider meshes $\mathcal{T}_h$ that are aligned with the fracture Γ, so that any element $E \in \mathcal{T}_h$ cannot be cut by Γ and it belongs exactly to one of the two disjoint subdomains Ω_1 or Ω_2. This implies that each mesh $\mathcal{T}_h$ induces a subdivision of the fracture Γ into faces, which we denote by Γ_h. It follows that we can write

$$\mathcal{F}_h = \mathcal{F}_h^I \cup \mathcal{F}_h^B \cup \Gamma_h,$$

where $\mathcal{F}_h^B$ is the set of faces lying on the boundary of the domain $\partial\Omega$ and $\mathcal{F}_h^I$ is the set of interior faces not belonging to the fracture. In addition, we write $\mathcal{F}_h^B = \mathcal{F}_h^D \cup \mathcal{F}_h^N$, where $\mathcal{F}_h^D$ and $\mathcal{F}_h^N$ are the boundary faces contained in $\partial\Omega_D$ and $\partial\Omega_N$, respectively (we assume the decomposition to be matching with the partition of $\partial\Omega$ into $\partial\Omega_D$ and $\partial\Omega_N$).

The induced discretization of the fracture Γ_h consists of the faces of the elements of $\mathcal{T}_h$ that share part of their boundary with the fracture, so that Γ_h is made up of line segments when $d = 2$ and of triangles when $d = 3$. Note that, in the $3D$ case, the triangles are not necessarily shape-regular and they may present hanging nodes, due to the fact that the sub-triangulations of each elemental interface is chosen independently from the others. For this reason, we extend the concept of *interface* also to the $(d-2)$-dimensional facets of elements in Γ_h, defined again as intersection of boundaries of two neighbouring elements. When $d = 2$, the interfaces reduce to points, while when $d = 3$ they consists of line segments. We denote by $\mathcal{E}_{\Gamma,h}$ the set of all the interfaces (that we will also call edges) of the elements in Γ_h, and we write, accordingly to the previous notation, $\mathcal{E}_{\Gamma,h} = \mathcal{E}_{\Gamma,h}^I \cup \mathcal{E}_{\Gamma,h}^B$, with $\mathcal{E}_{\Gamma,h}^B = \mathcal{E}_{\Gamma,h}^D \cup \mathcal{E}_{\Gamma,h}^N$.

For each element $E \in \mathcal{T}_h$, we denote by $|E|$ its measure, by h_E its diameter and we set $h = \max_{E\in\mathcal{T}_h} h_E$. Given an element $E \in \mathcal{T}_h$, for any face $F \subset \partial E$, with $F \in \mathcal{F}_h$, we define $\mathbf{n}_F$ as the unit normal vector on F that points outward of E. We can then define the standard jump and average operators across a face $F \in \mathcal{F}_h \setminus \mathcal{F}_h^B$ for (regular enough) scalar and vector-valued functions similarly to (1). We also recall a well-known identity [19] for scalar and vector-valued functions q and $\mathbf{v}$ that are piecewise smooth on $\mathcal{T}_h$:

$$\sum_{E\in\mathcal{T}_h} \int_{\partial E} q\mathbf{v}\cdot\mathbf{n}_E = \int_{\mathcal{F}_h} \{\mathbf{v}\}\cdot[\![q]\!] + \int_{\mathcal{F}_h\setminus\mathcal{F}_h^B} [\![\mathbf{v}]\!]\{q\}, \tag{8}$$

where we have used the compact notation $\int_{\mathcal{F}_h} \cdot = \sum_{F\in\mathcal{F}_h} \int_F \cdot$ and jump and average operators on a boundary face $F \in \mathcal{F}_h^B$ are defined as $[\![q]\!] = q\mathbf{n}_F$ and $\{\mathbf{v}\} = \mathbf{v}$.

Analogous definitions may be also set up on the fracture. In particular, given an element $F \in \Gamma_h$, with measure $|F|$ and diameter h_F, for any edge $e \subset \partial F$, with $e \in \mathcal{E}_{\Gamma,h}$, we define $\mathbf{n}_e$ as the unit normal vector on e pointing outward of F (it reduces to ± 1 when $d = 2$). Finally, standard jump and average operators across every edge e can be defined for (regular enough) scalar and vector-valued functions and an analogous version of formula (8) can be stated for piecewise smooth function on the fracture mesh Γ_h.
We have now all the ingredients to introduce the discrete formulation of model problem (7).

3.1 Discrete formulation

For simplicity in the forthcoming analysis, we will suppose that the permeability tensors $\boldsymbol{\nu}$ and $\boldsymbol{\nu}_\Gamma$ are piecewise *constant* on mesh elements, i.e., $\boldsymbol{\nu}|_E \in [\mathbb{P}_0(E)]^{d\times d}$ for all $E \in \mathcal{T}_h$,

and $\boldsymbol{\nu}_\Gamma|_F \in [\mathbb{P}_0(F)]^{(d-1)\times(d-1)}$ for all $F \in \Gamma_h$. First, we introduce the finite-dimensional spaces where we will set our discrete problem. We set

$$\begin{aligned} Q_h^b &= \{q \in L^2(\Omega) : \ q|_E \in \mathbb{P}_{k_E}(E) \ \forall E \in \mathcal{T}_h\} \\ \mathbf{W}_h^b &= \{\mathbf{v} \in [L^2(\Omega)]^d : \ \mathbf{v}|_E \in [\mathbb{P}_{k_E}(E)]^d \ \forall E \in \mathcal{T}_h\} \\ Q_h^\Gamma &= \{q_\Gamma \in L^2(\Gamma) : \ q_\Gamma|_F \in \mathbb{P}_{k_F}(F) \ \forall F \in \Gamma_h\} \\ \mathbf{W}_h^\Gamma &= \{\mathbf{v}_\Gamma \in [L^2(\Gamma)]^{d-1} : \ \mathbf{v}_\Gamma|_F \in [\mathbb{P}_{k_F}(F)]^{d-1} \ \forall F \in \Gamma_h\}. \end{aligned}$$

Note that, to each element $E \in \mathcal{T}_h$ is associated the polynomial degree $k_E \geq 1$, as well as to each face $F \in \Gamma_h$ is associated the degree $k_F \geq 1$. We remark that the polynomial degrees in the bulk and fracture discrete spaces just defined are chosen *independently* of each other.

We first focus on the problem in the bulk. Multiplying the first and second equations in (2) by test functions $\mathbf{v} \in \mathbf{W}_h^b$ and $q \in Q_h^b$, respectively, and integrating by parts over an element $E \in \mathcal{T}_h$, we obtain

$$\begin{aligned} \int_E \boldsymbol{\nu}^{-1}\mathbf{u}\cdot\mathbf{v} &= -\int_E p\nabla\cdot\mathbf{v} + \int_{\partial E} p\mathbf{v}\cdot\mathbf{n}_E, \\ \int_E \mathbf{u}\cdot\nabla q &= \int_{\partial E} q\,\mathbf{u}\cdot\mathbf{n}_E + \int_E fq. \end{aligned}$$

In the spirit of [20], we start the derivation of our DG discretization from these equations. Adding over the elements $E \in \mathcal{T}_h$, the general discrete formulation for the problem in the bulk will then be: Find $p_h \in Q_h^b$ and $\mathbf{u}_h \in \mathbf{W}_h^b$, such that for all $E \in \mathcal{T}_h$ we have

$$\begin{aligned} \sum_{E\in\mathcal{T}_h}\int_E \boldsymbol{\nu}^{-1}\mathbf{u}_h\cdot\mathbf{v} &= -\sum_{E\in\mathcal{T}_h}\int_E p_h\,\nabla\cdot\mathbf{v} + \sum_{E\in\mathcal{T}_h}\int_{\partial E}\widehat{p}_E\mathbf{v}\cdot\mathbf{n}_E \\ \sum_{E\in\mathcal{T}_h}\int_E \mathbf{u}_h\cdot\nabla q &= \sum_{E\in\mathcal{T}_h}\int_{\partial E} q\,\widehat{\mathbf{u}}_E\cdot\mathbf{n}_E + \sum_{E\in\mathcal{T}_h}\int_E fq, \end{aligned}$$

where the *numerical fluxes* $\widehat{p}_E$ and $\widehat{\mathbf{u}}_E$ are approximations to the exact solutions $\mathbf{u}$ and p, respectively, on the boundary of E. The definition of the numerical fluxes in terms of p_h, $\mathbf{u}_h$, of the boundary data and of the coupling conditions (5a)-(5b) will determine the method. Using identity (8), we get

$$\int_{\mathcal{T}_h}\boldsymbol{\nu}^{-1}\mathbf{u}_h\cdot\mathbf{v} = -\int_{\mathcal{T}_h} p_h\nabla\cdot\mathbf{v} + \int_{\mathcal{F}_h^I\cup\Gamma_h}\{\widehat{p}\}[\![\mathbf{v}]\!] + \int_{\mathcal{F}_h^I\cup\mathcal{F}_h^B\cup\Gamma_h}[\![\widehat{p}]\!]\cdot\{\mathbf{v}\}, \tag{9}$$

$$\int_{\mathcal{T}_h}\mathbf{u}_h\cdot\nabla q - \int_{\mathcal{F}_h^I\cup\mathcal{F}_h^B\cup\Gamma_h}\{\widehat{\mathbf{u}}\}\cdot[\![q]\!] - \int_{\mathcal{F}_h^I\cup\Gamma_h}[\![\widehat{\mathbf{u}}]\!]\{q\} = \int_{\mathcal{T}_h} fq, \tag{10}$$

where we have introduced $\hat{p} = (\hat{p}_E)_{E\in\mathcal{T}_h}$ and $\hat{\mathbf{u}} = (\hat{\mathbf{u}}_E)_{E\in\mathcal{T}_h}$. The numerical fluxes $\hat{p}$ and $\hat{\mathbf{u}}$ must be interpreted as linear functionals taking values in the spaces $\Pi_{E\in\mathcal{T}_h}L^2(\partial E)$ and $[\Pi_{E\in\mathcal{T}_h}L^2(\partial E)]^d$, respectively. In particular, this means that they are, in general, double-valued on $\mathcal{F}_h^I\cup\Gamma_h$ and single-valued on $\mathcal{F}_h^B$. We also observe for future use that, after integrating by parts and using again identity (8), equation (9) may also be rewritten as

$$\int_{\mathcal{T}_h}\boldsymbol{\nu}^{-1}\mathbf{u}_h\cdot\mathbf{v} = \int_{\mathcal{T}_h}\nabla p_h\cdot\mathbf{v} + \int_{\mathcal{F}_h^I\cup\Gamma_h}\{\widehat{p}-p_h\}[\![\mathbf{v}]\!] + \int_{\mathcal{F}_h^I\cup\mathcal{F}_h^B\cup\Gamma_h}[\![\widehat{p}-p_h]\!]\cdot\{\mathbf{v}\}. \tag{11}$$

We now reason analogously for the fracture. Multiplying the first and second equations in (4) by test functions $\mathbf{v}_\Gamma$ and q_Γ, respectively, integrating by parts over an element $F \in \Gamma_h$ and summing over all the elements in Γ_h we obtain the following problem: Find $p_{\Gamma,h} \in Q_h^\Gamma$ and $\mathbf{u}_{\Gamma,h} \in \mathbf{W}_h^\Gamma$ such that for all $F \in \Gamma_h$ we have

$$\sum_{F\in\Gamma_h}\int_F (\boldsymbol{\nu}_\Gamma^\tau \ell_\Gamma)^{-1}\mathbf{u}_{\Gamma,h}\cdot\mathbf{v}_\Gamma = -\sum_{F\in\Gamma_h}\int_F p_{\Gamma,h}\nabla\cdot\mathbf{v}_\Gamma + \sum_{F\in\Gamma_h}\int_{\partial F}\widehat{p}_{\Gamma,F}\mathbf{v}\cdot\mathbf{n}_F,$$
$$\sum_{F\in\Gamma_h}\int_F \mathbf{u}_{\Gamma,h}\cdot\nabla q_\Gamma - \sum_{F\in\Gamma_h}\int_{\partial F} q_\Gamma\widehat{\mathbf{u}}_{\Gamma,F}\cdot\mathbf{n}_F = \sum_{F\in\Gamma_h}\int_F f_\Gamma q_\Gamma - \sum_{F\in\Gamma_h}\int_F [\![\mathbf{u}]\!] q_\Gamma.$$

Here, we have introduced the numerical fluxes $\widehat{p}_{\Gamma,F}$ and $\widehat{\mathbf{u}}_{\Gamma,F}$. Again, the idea is that they represent approximations on the boundary of the fracture face F of the exact solutions p_Γ and $\mathbf{u}_\Gamma$, respectively. Note also that here $\mathbf{u}$ is the exact solution in the bulk. Using identity (8), we get

$$\int_{\Gamma_h}(\boldsymbol{\nu}_\Gamma^\tau\ell_\Gamma)^{-1}\mathbf{u}_{\Gamma,h}\cdot\mathbf{v}_\Gamma = -\sum_{F\in\Gamma_h}\int_F p_{\Gamma,h}\nabla\cdot\mathbf{v}_\Gamma + \int_{\mathcal{E}^I_{h,\Gamma}}\{\widehat{p}_\Gamma\}[\![\mathbf{v}_\Gamma]\!] + \int_{\mathcal{E}_{h,\Gamma}}\{\mathbf{v}_\Gamma\}\cdot[\![\widehat{p}_\Gamma]\!] \quad (12)$$
$$\int_{\Gamma_h}\mathbf{u}_{\Gamma,h}\cdot\nabla q_\Gamma - \int_{\mathcal{E}^I_{\Gamma,h}}\{q_\Gamma\}[\![\widehat{\mathbf{u}}_\Gamma]\!] - \int_{\mathcal{E}_{\Gamma,h}}\{\widehat{\mathbf{u}}_\Gamma\}\cdot[\![q_\Gamma]\!] = \int_{\Gamma_h} f_\Gamma q_\Gamma - \int_{\Gamma_h}[\![\mathbf{u}]\!] q_\Gamma \quad (13)$$

We point out that, in all previous equations, the gradient and divergence operators are actually *tangent* operators. Here, we have dropped the subscript τ in order to simplify the notation.

In the following, we explore all possible combinations of primal-primal, mixed-primal, primal mixed and mixed-mixed formulations for the bulk and fracture, respectively.

Primal-Primal formulation

In order to obtain the primal-primal formulation, we need to eliminate the velocities $\mathbf{u}_h$ and $\mathbf{u}_{\Gamma,h}$ from equations (9)-(10) and (12)-(13). To do so, we need to express $\mathbf{u}_h$ solely in terms of p_h (and $p_{\Gamma,h}$), and $\mathbf{u}_{\Gamma,h}$ solely in terms of $p_{\Gamma,h}$. As in [20] this will be achieved via the definition of proper *lifting operators*.

We start by focusing on the problem in the bulk. In order to complete the specification of the DG method that we want to use for the approximation, we need to give an expression to the numerical fluxes. We choose the classic *symmetric interior penalty* method (SIPDG). Moreover, coupling conditions (5a)-(5b) are imposed through a suitable definition of the numerical fluxes on the fracture faces. Since we want a primal formulation, the definition of

$\hat{p}$ and $\hat{\mathbf{u}}$ will not contain $\mathbf{u}_h$. The numerical fluxes are defined as follows:

$$\hat{p} = \hat{p}(p_h) = \begin{cases} \{p_h\} & \text{on } \mathcal{F}_h^I \\ g_D & \text{on } \mathcal{F}_h^D \\ p_h & \text{on } \mathcal{F}_h^N \\ p_h & \text{on } \Gamma_h \end{cases}$$

$$\hat{\mathbf{u}} = \hat{\mathbf{u}}(p_h, p_{\Gamma,h}) = \begin{cases} \{\boldsymbol{\nu}\nabla p_h\} - \sigma_F[\![p_h]\!] & \text{on } \mathcal{F}_h^I \\ \boldsymbol{\nu}\nabla p_h - \sigma_F(p_h - g_D)\mathbf{n}_F & \text{on } \mathcal{F}_h^D \\ 0 & \text{on } \mathcal{F}_h^N \\ -[\alpha_\Gamma(\{p_h\} - p_{\Gamma,h})\frac{\mathbf{n}_E}{2} + \beta_\Gamma[\![p_h]\!]] & \text{on } \Gamma_h \end{cases} \tag{14}$$

Here, we have introduced the discontinuity penalization parameter σ. In particular, σ is a non-negative bounded function, i.e., $\sigma \in L^\infty(\mathcal{F}_h^I \cup \mathcal{F}_h^D)$ and its precise definition will be given in Definition 4.2 below. Moreover, we have used the notation $\sigma_F = \sigma|_F$, for $F \in \mathcal{F}_h^I \cup \mathcal{F}_h^D$. We remark that, with this choice, the numerical flux $\hat{p}$ is doubled valued on Γ_h and single valued on $\mathcal{F}_h^I \cup \mathcal{F}_h^B$.
Using the definition of the numerical fluxes, it follows that

$$\begin{aligned}
&\{\hat{p} - p_h\} = 0, && [\![\hat{\mathbf{u}}]\!] = 0 && \text{on } \mathcal{F}_h^I, \\
&\{\hat{p} - p_h\} = 0, && [\![\hat{\mathbf{u}}]\!] = -\alpha_\Gamma(\{p_h\} - p_{\Gamma,h}) && \text{on } \Gamma_h, \\
&[\![\hat{p} - p_h]\!] = -[\![p_h]\!], && \{\hat{\mathbf{u}}\} = \{\boldsymbol{\nu}\nabla p_h\} - \sigma_F[\![p_h]\!] && \text{on } \mathcal{F}_h^I, \\
&[\![\hat{p} - p_h]\!] = (g_D - p_h)\mathbf{n}_F, && \{\hat{\mathbf{u}}\} = \boldsymbol{\nu}\nabla p_h - \sigma_F(p_h - g_D)\mathbf{n}_F && \text{on } \mathcal{F}_h^D, \\
&[\![\hat{p} - p_h]\!] = 0, && \{\hat{\mathbf{u}}\} = 0 && \text{on } \mathcal{F}_h^N, \\
&[\![\hat{p} - p_h]\!] = 0, && \{\hat{\mathbf{u}}\} = -\beta_\Gamma[\![p_h]\!] && \text{on } \Gamma_h,
\end{aligned}$$

so we rewrite (11) as

$$\int_{\mathcal{T}_h} \boldsymbol{\nu}^{-1}\mathbf{u}_h \cdot \mathbf{v} = \int_{\mathcal{T}_h} \nabla p_h \cdot \mathbf{v} - \int_{\mathcal{F}_h^I \cup \mathcal{F}_h^D} [\![p_h]\!] \cdot \{\mathbf{v}\} + \int_{\mathcal{F}_h^D} g_D \mathbf{v} \cdot \mathbf{n}. \tag{15}$$

At this point, we proceed with the elimination of the auxiliary variable $\mathbf{u}_h$ from our equations. To this aim, we introduce the *lifting operator* $\mathscr{L}_b^{SIP} : [L^1(\mathcal{F}_h^I \cup \mathcal{F}_h^D)]^d \to \mathbf{W}_h^b$ defined by

$$\int_{\mathcal{T}_h} \mathscr{L}_b^{SIP}(\boldsymbol{\xi}) \cdot \mathbf{v} = -\int_{\mathcal{F}_h^I \cup \mathcal{F}_h^D} \{\mathbf{v}\} \cdot \boldsymbol{\xi} \quad \forall \mathbf{v} \in \mathbf{W}_h^b. \tag{16}$$

Similarly, we define the lifting $\mathcal{G}_b(g_D) \in \mathbf{W}_h^b$ of the Dirichlet boundary datum g_D as

$$\int_{\mathcal{T}_h} \mathcal{G}_b \cdot \mathbf{v} = \int_{\mathcal{F}_h^D} g_D \mathbf{v} \cdot \mathbf{n} \quad \forall \mathbf{v} \in \mathbf{W}_h^b. \tag{17}$$

Thanks to the introduction of the lifting operators, equation (15) may be rewritten as

$$\int_{\mathcal{T}_h} \Big(\mathbf{u}_h - \boldsymbol{\nu}[\nabla p_h + \mathscr{L}_b^{SIP}([\![p_h]\!]) + \mathcal{G}_b]\Big) \cdot \mathbf{v} = 0.$$

Since $\nabla Q_h^b \subseteq \mathbf{W}_h^b$, we can write

$$\mathbf{u}_h = \boldsymbol{\nu}[\nabla p_h + \mathscr{L}_b^{SIP}([\![p_h]\!]) + \mathcal{G}_b], \tag{18}$$

where $\nabla p_h + \mathscr{L}_b^{SIP}([\![p_h]\!]) + \mathcal{G}_b$ can be seen as a discrete approximation of the gradient ∇p.

We can then rewrite equation (10) as

$$\int_{\mathcal{T}_h} \boldsymbol{\nu}[\nabla p_h + \mathscr{L}_b^{SIP}([\![p_h]\!]) + \mathcal{G}_b] \cdot \nabla q - \int_{\mathcal{F}_h^I \cup \mathcal{F}_h^B \cup \Gamma_h} \{\widehat{\mathbf{u}}\} \cdot [\![q]\!] - \int_{\mathcal{F}_h^I \cup \Gamma_h} [\![\widehat{\mathbf{u}}]\!]\{q\} = \int_{\mathcal{T}_h} fq.$$

Using the definition of the discrete gradient (18), of the lifting operators (16) and (17) and of the numerical flux $\hat{\mathbf{u}}$ (14), we have

$$\begin{aligned}\int_{\mathcal{T}_h} \boldsymbol{\nu}\nabla p_h \cdot \nabla q + \int_{\mathcal{T}_h} \boldsymbol{\nu}\mathscr{L}_b^{SIP}([\![p_h]\!]) \cdot \nabla q + \int_{\mathcal{T}_h} \boldsymbol{\nu}\mathscr{L}_b^{SIP}([\![q]\!]) \cdot \nabla p_h + \int_{\mathcal{F}_h^I \cup \mathcal{F}_h^D} \sigma_F [\![p_h]\!] \cdot [\![q]\!] \\ + \int_{\Gamma_h} \beta_\Gamma [\![p_h]\!] \cdot [\![q]\!] + \int_{\Gamma_h} \alpha_\Gamma (\{p_h\} - p_{\Gamma,h})\{q\} \\ = \int_{\mathcal{T}_h} fq + \int_{\mathcal{F}_h^D} g_D \sigma_F q - \int_{\mathcal{T}_h} \boldsymbol{\nu}\mathcal{G}_b \cdot \nabla q. \end{aligned} \tag{19}$$

Now we move our attention to the problem in the fracture. We define the numerical fluxes $\hat{p}_\Gamma$ and $\hat{\mathbf{u}}_\Gamma$ in order to obtain a symmetric interior penalty approximation as follows:

$$\hat{p}_\Gamma = \hat{p}_\Gamma(p_{\Gamma,h}) = \begin{cases} \{p_{\Gamma,h}\} & \text{on } \mathcal{E}_{\Gamma,h}^I \\ g_\Gamma & \text{on } \mathcal{E}_{\Gamma,h}^D \\ p_{\Gamma,h} & \text{on } \mathcal{E}_{\Gamma,h}^N, \end{cases}$$

$$\hat{\mathbf{u}}_\Gamma = \hat{\mathbf{u}}_\Gamma(p_{\Gamma,h}) = \begin{cases} \{\boldsymbol{\nu}_\Gamma^\tau \ell_\Gamma \nabla p_{\Gamma,h}\} - \sigma_e [\![p_{\Gamma,h}]\!] & \text{on } \mathcal{E}_{\Gamma,h}^I \\ \boldsymbol{\nu}_\Gamma^\tau \ell_\Gamma \nabla p_{\Gamma,h} - \sigma_e (p_{\Gamma,h} - g_\Gamma)\mathbf{n}_e & \text{on } \mathcal{E}_{\Gamma,h}^D \\ 0 & \text{on } \mathcal{E}_{\Gamma,h}^N. \end{cases}$$

Again, we have introduced the discontinuity penalization parameter $\sigma_\Gamma \in L^\infty(\mathcal{E}_{\Gamma,h}^I \cup \mathcal{E}_{\Gamma,h}^D)$ and we set $\sigma_e = \sigma_\Gamma|_e$ for $e \in \mathcal{E}_{\Gamma,h}^I \cup \mathcal{E}_{\Gamma,h}^D$. Its precise definition will be given in Definition 4.3 below. Next, as before, we introduce the lifting operator $\mathscr{L}_\Gamma^{SIP} : [L^1(\mathcal{E}_{\Gamma,h}^I \cup \mathcal{E}_{\Gamma,h}^D)]^{d-1} \to \mathbf{W}_h^\Gamma$ and the lifting of the boundary datum $\mathcal{G}_\Gamma(g_{\Gamma,D}) \in \mathbf{W}_h^\Gamma$ defined by

$$\int_{\Gamma_h} \mathscr{L}_\Gamma^{SIP}(\boldsymbol{\xi}_\Gamma) \cdot \mathbf{v}_\Gamma = -\int_{\mathcal{E}_{\Gamma,h}^I \cup \mathcal{E}_{\Gamma,h}^D} \boldsymbol{\xi}_\Gamma \cdot \{\mathbf{v}_\Gamma\} \qquad \forall \mathbf{v}_\Gamma \in \mathbf{W}_h^\Gamma, \tag{20}$$

$$\int_{\Gamma_h} \mathcal{G}_\Gamma \cdot \mathbf{v}_\Gamma = \int_{\mathcal{E}_{\Gamma,h}^D} g_{\Gamma,D} \mathbf{v}_\Gamma \cdot \mathbf{n}_\tau \qquad \forall \mathbf{v}_\Gamma \in \mathbf{W}_h^\Gamma. \tag{21}$$

Integrating by parts and using (8), we can rewrite equation (12) as

$$\int_{\Gamma_h} \Big(\mathbf{u}_{\Gamma,h} - \boldsymbol{\nu}_\Gamma^\tau \ell_\Gamma [\nabla p_{\Gamma,h} + \mathscr{L}_\Gamma^{SIP}([\![p_{\Gamma,h}]\!]) + \mathcal{G}_\Gamma] \Big) \cdot \mathbf{v}_\Gamma = 0.$$

Again, since $\nabla Q_h^\Gamma \subseteq \mathbf{W}_h^\Gamma$ elementwise, we can write

$$\mathbf{u}_{\Gamma,h} = \boldsymbol{\nu}_\Gamma^\tau \ell_\Gamma [\nabla p_{\Gamma,h} + \mathscr{L}_\Gamma^{SIP}([\![p_{\Gamma,h}]\!]) + \mathcal{G}_\Gamma].$$

Plugging this last identity and the definition of the numerical flux $\hat{\mathbf{u}}_\Gamma$ into equation (13) and using the coupling conditions to substitute $-[\![\mathbf{u}]\!] = \alpha_\Gamma(\{p_h\} - p_{\Gamma,h})$, we obtain

$$\begin{aligned}\int_{\Gamma_h} \boldsymbol{\nu}_\Gamma^\tau \ell_\Gamma \nabla p_{\Gamma,h} \cdot \nabla q_\Gamma + \int_{\Gamma_h} \boldsymbol{\nu}_\Gamma^\tau \ell_\Gamma \mathscr{L}_\Gamma^{SIP}([\![p_{\Gamma,h}]\!]) \cdot \nabla q_\Gamma + \int_{\Gamma_h} \boldsymbol{\nu}_\Gamma^\tau \ell_\Gamma \mathscr{L}_\Gamma^{SIP}([\![q_\Gamma]\!]) \cdot \nabla p_{\Gamma,h} \\ + \int_{\mathcal{E}_{\Gamma,h}^I \cup \mathcal{E}_{\Gamma,h}^D} \sigma_e [\![p_{\Gamma,h}]\!] \cdot [\![q_\Gamma]\!] + \int_{\Gamma_h} \alpha_\Gamma p_{\Gamma,h} q_\Gamma - \int_{\Gamma_h} \alpha_\Gamma \{p_h\} q_\Gamma \\ = \int_{\Gamma_h} f_\Gamma q_\Gamma + \int_{\mathcal{E}_{\Gamma,h}^D} g_\Gamma \sigma_e q_\Gamma - \int_{\Gamma_h} \boldsymbol{\nu}_\Gamma^\tau \ell_\Gamma \mathcal{G}_\Gamma \cdot \nabla q_\Gamma. \quad (22)\end{aligned}$$

In conclusion, summing equations (19) and (22) we obtain the following discrete formulation: Find $(p_h, p_h^\Gamma) \in Q_h^b \times Q_h^\Gamma$ such that

$$\mathcal{A}_h^{PP}\left((p_h, p_h^\Gamma), (q, q_\Gamma)\right) = \mathcal{L}_h^{PP}(q, q_\Gamma) \quad \forall (q, q_\Gamma) \in Q_h^b \times Q_h^\Gamma, \quad (23)$$

where PP stands for *primal-primal* and where $\mathcal{L}_h : Q_h^b \times Q_h^\Gamma \to \mathbb{R}$ is defined as $\mathcal{L}_h^{PP}(q, q_\Gamma) = \mathcal{L}_b^P(q) + \mathcal{L}_\Gamma^P(q_\Gamma)$ and $\mathcal{A}_h^{PP} : (Q_h^b \times Q_h^\Gamma) \times (Q_h^b \times Q_h^\Gamma) \to \mathbb{R}$ is defined as

$$\mathcal{A}_h^{PP}\left((p_h, p_h^\Gamma), (q, q_\Gamma)\right) = \mathcal{A}_b^P(p_h, q) + \mathcal{A}_\Gamma^P(p_{\Gamma,h}, q_\Gamma) + \mathcal{I}((p_h, p_{\Gamma,h}), (q, q_\Gamma)),$$

with

$$\begin{aligned}\mathcal{A}_b^P(p_h, q) = \int_{\mathcal{T}_h} \boldsymbol{\nu} \nabla p_h \cdot \nabla q + \int_{\mathcal{T}_h} \boldsymbol{\nu} \mathscr{L}_b^{SIP}([\![p_h]\!]) \cdot \nabla q \\ + \int_{\mathcal{T}_h} \boldsymbol{\nu} \mathscr{L}_b^{SIP}([\![q]\!]) \cdot \nabla p_h + \int_{\mathcal{F}_h^I \cup \mathcal{F}_h^D} \sigma_F [\![p_h]\!] \cdot [\![q]\!], \quad (24)\\ \mathcal{A}_\Gamma^P(p_{\Gamma,h}, q_\Gamma) = \int_{\Gamma_h} \boldsymbol{\nu}_\Gamma^\tau \ell_\Gamma \nabla p_{\Gamma,h} \cdot \nabla q_\Gamma + \int_{\Gamma_h} \boldsymbol{\nu}_\Gamma^\tau \ell_\Gamma \mathscr{L}_\Gamma^P([\![p_{\Gamma,h}]\!]) \cdot \nabla q_\Gamma \\ + \int_{\Gamma_h} \boldsymbol{\nu}_\Gamma^\tau \ell_\Gamma \mathscr{L}_\Gamma^{SIP}([\![q_\Gamma]\!]) \cdot \nabla p_{\Gamma,h} + \int_{\mathcal{E}_{\Gamma,h}^I \cup \mathcal{E}_{\Gamma,h}^D} \sigma_e [\![p_{\Gamma,h}]\!] \cdot [\![q_\Gamma]\!], \quad (25)\\ \mathcal{I}((p_h, p_{\Gamma,h}), (q, q_\Gamma)) = \int_{\Gamma_h} \beta_\Gamma [\![p_h]\!] \cdot [\![q]\!] + \int_{\Gamma_h} \alpha_\Gamma (\{p_h\} - p_{\Gamma,h})(\{q\} - q_{\Gamma,h}), \quad (26)\end{aligned}$$

and

$$\begin{aligned}\mathcal{L}_b^P(q) = \int_{\mathcal{T}_h} fq + \int_{\mathcal{F}_h^D} g_D \sigma_F q - \int_{\mathcal{T}_h} \boldsymbol{\nu} \mathcal{G}_b \cdot \nabla q, \quad (27)\\ \mathcal{L}_\Gamma^P(q_\Gamma) = \int_{\Gamma_h} f_\Gamma q_\Gamma + \int_{\mathcal{E}_{\Gamma,h}^D} g_\Gamma \sigma_e q_\Gamma - \int_{\Gamma_h} \boldsymbol{\nu}_\Gamma^\tau \ell_\Gamma \mathcal{G}_\Gamma \cdot \nabla q_\Gamma. \quad (28)\end{aligned}$$

We remark that we have recovered the formulation already obtained in [9] (in its not strongly consistent version), the only difference being that the bilinear form for the problem in the fracture is in the shape of SIPDG method, instead of classical conforming finite elements.

Mixed-Primal formulation

In this section, we discretize the problem in the bulk in its mixed form. To this aim, we use the local discontinuous Galerkin (LDG) method [46, 40, 63, 64]. The LDG method is a particular DG method that can be included in the class of mixed finite element methods. However, the variable $\mathbf{u}_h$ can be *locally* solved in terms of p_h and then eliminated from the equations, giving rise to a primal formulation with p_h as only unknown.

In what follows, we first derive the formulation of our method in a mixed setting. After that, we recast it in a primal setting, in order to perform the analysis in the framework of [20, 63]. However, we remark that the mixed formulation is the one that will actually be implemented for the numerical experiments of Section 6. As far as the problem in the fracture is concerned, we work again in a primal setting, using the SIPDG method for the discretization.

In the bulk, we define the numerical fluxes as

$$\hat{p} = \hat{p}(p_h) = \begin{cases} \{p_h\} + \mathbf{b} \cdot [\![p_h]\!] & \text{on } \mathcal{F}_h^I \\ g_D & \text{on } \mathcal{F}_h^D \\ p_h & \text{on } \mathcal{F}_h^N \\ p_h & \text{on } \Gamma_h \end{cases}$$

$$\hat{\mathbf{u}} = \hat{\mathbf{u}}(\mathbf{u}_h, p_h, p_{\Gamma,h}) = \begin{cases} \{\mathbf{u}_h\} - \mathbf{b}[\![\mathbf{u}_h]\!] - \sigma_F [\![p_h]\!] & \text{on } \mathcal{F}_h^I \\ \mathbf{u}_h - \sigma_F (p_h \mathbf{n}_F - g_D \mathbf{n}_F) & \text{on } \mathcal{F}_h^D \\ 0 & \text{on } \mathcal{F}_h^N \\ -[\alpha_\Gamma (\{p_h\} - p_{\Gamma,h}) \frac{\mathbf{n}_F}{2} + \beta_\Gamma [\![p_h]\!]] & \text{on } \Gamma_h \end{cases}$$

Here, $\mathbf{b} \in [L^\infty(\mathcal{F}_h^I)]^d$ is a (possibly null) vector-valued function which is constant on each face. It is chosen such that

$$||\mathbf{b}||_{\infty, \mathcal{F}_h^I} \leq B, \tag{29}$$

with $B \geq 0$ independent if the discretization parameters. Moreover, σ is the penalization parameter introduced in (14) , whose precise definition will be given in (48) below. Note that the numerical flux $\hat{p}$ does *not* depend on $\mathbf{u}_h$. This will allow for an element-by-element elimination of the variable $\mathbf{u}_h$, generating a primal formulation of the problem. We also point out that the definition of the numerical fluxes on the fracture faces is the same as in the primal SIPDG setting.

With this definition of the numerical fluxes, and after integration by parts as in (11), equation (9) becomes

$$\int_{\mathcal{T}_h} \boldsymbol{\nu}^{-1} \mathbf{u}_h \cdot \mathbf{v} - \int_{\mathcal{T}_h} \nabla p_h \cdot \mathbf{v} + \int_{\mathcal{F}_h^I} [\![p_h]\!] \cdot (\{\mathbf{v}\} - \mathbf{b}[\![\mathbf{v}]\!]) + \int_{\mathcal{F}_h^D} p_h \mathbf{v} \cdot \mathbf{n}_F = \int_{\mathcal{F}_h^D} g_D \mathbf{v} \cdot \mathbf{n}_F, \tag{30}$$

while equation (10) turns into

$$\begin{aligned} \int_{\mathcal{T}_h} \mathbf{u}_h \cdot \nabla q - \int_{\mathcal{F}_h^I} (\{\mathbf{u}_h\} - \mathbf{b}[\![\mathbf{u}_h]\!]) \cdot [\![q]\!] + \int_{\mathcal{F}_h^I \cup \mathcal{F}_h^D} \sigma_F [\![p_h]\!] \cdot [\![q]\!] - \int_{\mathcal{F}_h^D} q \mathbf{u}_h \cdot \mathbf{n}_F \\ + \int_{\Gamma_h} \beta_\Gamma [\![p_h]\!] \cdot [\![q]\!] + \int_{\Gamma_h} \alpha_\Gamma (\{p_h\} - p_{\Gamma,h}) \{q\} = \int_{\mathcal{T}_h} f q + \int_{\mathcal{F}_h^D} \sigma_F g_D q. \end{aligned} \tag{31}$$

If we discretize the problem in the fracture with the SIPDG method, we obtain the following discrete mixed problem: Find $\big((p_h, \mathbf{u}_h), p_h^\Gamma\big) \in Q_h^b \times \mathbf{W}_h^b \times Q_h^\Gamma$ such that

$$\begin{aligned} \mathcal{M}_b(\mathbf{u}_h, \mathbf{v}) + \mathcal{B}_b(p_h, \mathbf{v}) &= F_b(\mathbf{v}) && \forall \mathbf{v} \in \mathbf{W}_h^b, \\ -\mathcal{B}_b(q, \mathbf{u}_h) + \mathcal{S}_b(p_h, q) + \mathcal{I}_1(p_h, q, p_{\Gamma,h}) &= G_b(q) && \forall q \in Q_h^b, \\ \mathcal{A}_\Gamma^P(p_{\Gamma,h}, q_\Gamma) + \mathcal{I}_2(p_h, p_{\Gamma,h}, q_\Gamma) &= \mathcal{L}_\Gamma^P(q_\Gamma) && \forall q_\Gamma \in Q_h^\Gamma, \end{aligned} \tag{32}$$

where

$$\begin{aligned} \mathcal{M}_b(\mathbf{u}_h, \mathbf{v}) &= \int_{\mathcal{T}_h} \boldsymbol{\nu}^{-1}\mathbf{u}_h \cdot \mathbf{v}, \\ \mathcal{B}_b(p_h, \mathbf{v}) &= -\int_{\mathcal{T}_h} \nabla p_h \cdot \mathbf{v} + \int_{\mathcal{F}_h^I} [\![p_h]\!] \cdot (\{\mathbf{v}\} - \mathbf{b}[\![\mathbf{v}]\!]) + \int_{\mathcal{F}_h^D} p_h \mathbf{v} \cdot \mathbf{n}_F, \\ \mathcal{S}_b(p_h, q) &= \int_{\mathcal{F}_h^I \cup \mathcal{F}_h^D} \sigma_F [\![p_h]\!] \cdot [\![q]\!], \\ \mathcal{I}_1(p_h, q, p_{\Gamma,h}) &= \int_{\Gamma_h} \beta_\Gamma [\![p_h]\!] \cdot [\![q]\!] + \int_{\Gamma_h} \alpha_\Gamma (\{p_h\} - p_{\Gamma,h})\{q\}, \\ \mathcal{I}_2(p_h, p_{\Gamma,h}, q_\Gamma) &= \int_{\Gamma_h} \alpha_\Gamma (p_{\Gamma,h} - \{p_h\}) q_\Gamma, \\ F_b(\mathbf{v}) &= \int_{\mathcal{F}_h^D} g_D \mathbf{v} \cdot \mathbf{n}_F, \\ G_b(q) &= \int_{\mathcal{T}_h} fq + \int_{\mathcal{F}_h^D} \sigma_F g_D q, \end{aligned}$$

and $\mathcal{A}_\Gamma^P(\cdot,\cdot)$ and $\mathcal{L}_\Gamma^P(\cdot)$ are defined as in (25) and (28), respectively. Also note that we have $\mathcal{I}((p_h, p_{\Gamma,h}), (q, q_\Gamma)) = \mathcal{I}_1(p_h, q, p_{\Gamma,h}) + \mathcal{I}_2(p_h, p_{\Gamma,h}, q_\Gamma)$.

We now focus on rewriting the problem in the bulk in a primal form, taking advantage of the local solvability of LDG method. We proceed as in the SIPDG case and introduce an appropriate *lifting operator*, $\mathscr{L}_b^{LDG} : [L^1(\mathcal{F}_h^I \cup \mathcal{F}_h^D)]^d \to \mathbf{W}_h^b$, defined by

$$\int_{\mathcal{T}_h} \mathscr{L}_b^{LDG}(\boldsymbol{\xi}) \cdot \mathbf{v} = -\int_{\mathcal{F}_h^I} (\{\mathbf{v}\} - \mathbf{b}[\![\mathbf{v}]\!]) \cdot \boldsymbol{\xi} - \int_{\mathcal{F}_h^D} \boldsymbol{\xi} \cdot \mathbf{v} \quad \forall\, \mathbf{v} \in \mathbf{W}_h^b \tag{33}$$

From equation (30) we obtain

$$\mathbf{u}_h = \boldsymbol{\nu}(\nabla p_h + \mathscr{L}_b^{LDG}([\![p_h]\!]) + \mathcal{G}_b), \tag{34}$$

where $\mathcal{G}_b$ is the lifting of the Dirichlet boundary datum defined in (17). Equation (31) now becomes

$$\begin{aligned} &\int_{\mathcal{T}_h} \boldsymbol{\nu}\nabla p_h \cdot \nabla q + \int_{\mathcal{T}_h} \boldsymbol{\nu}\mathscr{L}_b^{LDG}([\![p_h]\!]) \cdot \nabla q_h + \int_{\mathcal{T}_h} \boldsymbol{\nu}\mathcal{G}_b \cdot \nabla q \\ &\quad - \int_{\mathcal{F}_h^I} (\{\mathbf{u}_h\} + \mathbf{b}[\![\mathbf{u}_h]\!]) \cdot [\![q]\!] - \int_{\mathcal{F}_h^D} q\mathbf{u}_h \cdot \mathbf{n}_F + \int_{\mathcal{F}_h^I \cup \mathcal{F}_h^D} \sigma_F [\![p_h]\!] \cdot [\![q]\!] \\ &\quad + \int_{\Gamma_h} \beta_\Gamma [\![p_h]\!] \cdot [\![q]\!] + \int_{\Gamma_h} \alpha_\Gamma (\{p_h\} - p_{\Gamma,h})\{q\} = \int_{\mathcal{T}_h} fq + \int_{\mathcal{F}_h^D} \sigma_F q g_D. \end{aligned}$$

Using again the definition of the lifting $\mathscr{L}_b^{LDG}$ and the identity (34), we obtain

$$\int_{\mathcal{T}_h} \boldsymbol{\nu}(\nabla p_h + \mathscr{L}_b^{LDG}([\![p_h]\!])) \cdot (\nabla q + \mathscr{L}_b^{LDG}([\![q]\!])) + \int_{\mathcal{F}_h^I \cup \mathcal{F}_h^D} \sigma_F [\![p_h]\!] \cdot [\![q]\!] + \int_{\Gamma_h} \beta_\Gamma [\![p_h]\!] \cdot [\![q]\!] + \int_{\Gamma_h} \alpha_\Gamma (\{p_h\} - p_\Gamma)\{q\} = \int_{\mathcal{T}_h} fq + \int_{\mathcal{F}_h^D} \sigma_F q g_D - \int_{\mathcal{T}_h} \boldsymbol{\nu} \mathcal{G}_b \cdot (\nabla q + \mathscr{L}_b^{LDG}([\![q]\!])). \quad (35)$$

Summing equations (35) and (22) we obtain the following discrete formulation: Find $(p_h, p_h^\Gamma) \in Q_h^b \times Q_h^\Gamma$ such that

$$\mathcal{A}_h^{MP}\left((p_h, p_h^\Gamma), (q, q_\Gamma)\right) = \mathcal{L}_h^{MP}(q, q_\Gamma) \quad \forall (q, q_\Gamma) \in Q_h^b \times Q_h^\Gamma, \quad (36)$$

where MP stands for *mixed-primal* and where $\mathcal{A}_h^{MP} : (Q_h^b \times Q_h^\Gamma) \times (Q_h^b \times Q_h^\Gamma) \to \mathbb{R}$ is defined as

$$\mathcal{A}_h^{MP}\left((p_h, p_h^\Gamma), (q, q_\Gamma)\right) = \mathcal{A}_b^M(p_h, q) + \mathcal{A}_\Gamma^P(p_{\Gamma,h}, q_\Gamma) + \mathcal{I}((p_h, p_{\Gamma,h}), (q, q_\Gamma)),$$

and $\mathcal{L}_h^{MP} : Q_h^b \times Q_h^\Gamma \to \mathbb{R}$ is defined as

$$\mathcal{L}_h^{MP}(q, q_\Gamma) = \mathcal{L}_b^M(q) + \mathcal{L}_\Gamma^P(q_\Gamma)$$

with

$$\mathcal{A}_b^M(p_h, q) = \int_{\mathcal{T}_h} \boldsymbol{\nu}(\nabla p_h + \mathscr{L}_b^{LDG}([\![p_h]\!])) \cdot (\nabla q + \mathscr{L}_b^{LDG}([\![q]\!])) + \int_{\mathcal{F}_h^I \cup \mathcal{F}_h^D} \sigma_F [\![p_h]\!] \cdot [\![q]\!] + \int_{\Gamma_h} \beta_\Gamma [\![p_h]\!] \cdot [\![q]\!] + \int_{\Gamma_h} \alpha_\Gamma (\{p_h\} - p_\Gamma)\{q\}, \quad (37)$$

$$\mathcal{L}_b^M(q) = \int_{\mathcal{T}_h} fq + \int_{\mathcal{F}_h^D} \sigma_F q g_D - \int_{\mathcal{T}_h} \boldsymbol{\nu} \mathcal{G}_b \cdot (\nabla q + \mathscr{L}_b^{LDG}([\![q]\!])).$$

Note that the mixed formulation (32) is equivalent to the primal formulation (36) together with the definition of the lifting operator (33) and equation (34).

Primal-Mixed formulation

We now want to approximate the problem in the fracture in mixed form, employing the LDG method and the problem in the bulk using the SIPDG method. We define the numerical fluxes as follows

$$\hat{p}_\Gamma = \hat{p}_\Gamma(p_{\Gamma,h}) = \begin{cases} \{p_{\Gamma,h}\} + \mathbf{b}_\Gamma \cdot [\![p_{\Gamma,h}]\!] & \text{on } \mathcal{E}_{\Gamma,h}^I \\ g_\Gamma & \text{on } \mathcal{E}_{\Gamma,h}^D \\ p_{\Gamma,h} & \text{on } \mathcal{E}_{\Gamma,h}^N \end{cases}$$

$$\hat{\mathbf{u}}_\Gamma = \hat{\mathbf{u}}_\Gamma(\mathbf{u}_{\Gamma,h}, p_{\Gamma,h}) = \begin{cases} \{\mathbf{u}_{\Gamma,h}\} - \mathbf{b}_\Gamma [\![\mathbf{u}_{\Gamma,h}]\!] - \sigma_e [\![p_{\Gamma,h}]\!] & \text{on } \mathcal{E}_{\Gamma,h}^I \\ \mathbf{u}_{\Gamma,h} - \sigma_e (p_{\Gamma,h}\mathbf{n}_e - g_\Gamma \mathbf{n}_e) & \text{on } \mathcal{E}_{\Gamma,h}^D \\ 0 & \text{on } \mathcal{E}_{\Gamma,h}^N \end{cases}$$

Here, $\mathbf{b}_\Gamma \in [L^\infty(\mathcal{E}^I_{\Gamma,h})]^{d-1}$ is a vector-valued function that is constant on each edge and it is chosen such that $||\mathbf{b}_\Gamma||_{\infty,\mathcal{E}^I_{\Gamma,h}} \leq B_\Gamma$, with $B_\Gamma \leq 0$ independent of the discretization parameters. Equations (12) and (13) now become

$$\int_{\Gamma_h} (\boldsymbol{\nu}_\Gamma^\tau \ell_\Gamma)^{-1} \mathbf{u}_{\Gamma,h} \cdot \mathbf{v}_\Gamma - \int_{\Gamma_h} \mathbf{v}_\Gamma \cdot \nabla p_{\Gamma,h} + \int_{\mathcal{E}^I_{h,\Gamma}} [\![p_{\Gamma,h}]\!] \cdot (\{\mathbf{v}_\Gamma\} - \mathbf{b}_\Gamma [\![\mathbf{v}_\Gamma]\!]) + \int_{\mathcal{E}^D_{h,\Gamma}} p_{\Gamma,h} \mathbf{v}_\Gamma \cdot \mathbf{n}_e = \int_{\mathcal{E}^D_{h,\Gamma}} g_\Gamma \mathbf{v}_\Gamma \cdot \mathbf{n}_e \quad (38)$$

$$\int_{\Gamma_h} \mathbf{u}_{\Gamma,h} \cdot \nabla q_\Gamma - \int_{\mathcal{E}^I_{\Gamma,h}} [\![q_\Gamma]\!] \cdot (\{\mathbf{u}_{\Gamma,h}\} - \mathbf{b}_\Gamma [\![\mathbf{u}_{\Gamma,h}]\!]) + \int_{\mathcal{E}_{\Gamma,h}} \sigma_e [\![p_{\Gamma,h}]\!] \cdot [\![q_\Gamma]\!] - \int_{\mathcal{E}^D_{\Gamma,h}} q_\Gamma \mathbf{u}_{\Gamma,h} \cdot \mathbf{n}_e = \int_{\Gamma_h} f_\Gamma q_\Gamma + \int_{\Gamma_h} \alpha_\Gamma(\{p_h - p_{\Gamma,h}\}) q_\Gamma + \int_{\mathcal{E}_{\Gamma,h}} \sigma_e g_\Gamma q_\Gamma, \quad (39)$$

where we have also used the coupling conditions to write $-[\![\mathbf{u}]\!] = \alpha_\Gamma(\{p_h\} - p_{\Gamma,h}) q_\Gamma$ For the bulk we proceed as in the primal-primal section using for the discretization the SIPDG method. We then obtain the following primal-mixed problem: Find $\big(p_h, (p_h^\Gamma, \mathbf{u}_{\Gamma,h})\big) \in Q_h^b \times Q_h^\Gamma \times \mathbf{W}_h^\Gamma$ such that

$$\begin{aligned} \mathcal{A}_b^P(p_h, q) + \mathcal{I}_1((p_h, q), p_{\Gamma,h}) &= \mathcal{L}_b^P(q) \quad && \forall q \in Q_h^b \\ \mathcal{M}_\Gamma(\mathbf{u}_{\Gamma,h}, \mathbf{v}_\Gamma) + \mathcal{B}_\Gamma(p_{\Gamma,h}, \mathbf{v}_\Gamma) &= F_\Gamma(\mathbf{v}_\Gamma) \quad && \forall \mathbf{v}_\Gamma \in \mathbf{W}_h^\Gamma, \\ -\mathcal{B}_\Gamma(q_\Gamma, \mathbf{u}_{\Gamma,h}) + \mathcal{S}_\Gamma(p_{\Gamma,h}, q_\Gamma) + \mathcal{I}_2(p_h, (p_{\Gamma,h}, q_\Gamma)) &= G_\Gamma(q_\Gamma) \quad && \forall q_\Gamma \in Q_h^\Gamma, \end{aligned} \quad (40)$$

where

$$\begin{aligned} \mathcal{M}_\Gamma(\mathbf{u}_{\Gamma,h}, \mathbf{v}_\Gamma) &= \int_{\Gamma_h} (\boldsymbol{\nu}_\Gamma^\tau \ell_\Gamma)^{-1} \mathbf{u}_{\Gamma,h} \cdot \mathbf{v}_\Gamma, \\ \mathcal{B}_\Gamma(p_{\Gamma,h}, \mathbf{v}_\Gamma) &= -\int_{\Gamma_h} \mathbf{v}_\Gamma \cdot \nabla p_{\Gamma,h} + \int_{\mathcal{E}^I_{h,\Gamma}} [\![p_{\Gamma,h}]\!] \cdot (\{\mathbf{v}_\Gamma\} - \mathbf{b}_\Gamma [\![\mathbf{v}_\Gamma]\!]) + \int_{\mathcal{E}^D_{h,\Gamma}} p_{\Gamma,h} \mathbf{v}_\Gamma \cdot \mathbf{n}_e, \\ \mathcal{S}_b(p_{\Gamma,h}, q_\Gamma) &= \int_{\mathcal{E}_{\Gamma,h}} \sigma_e [\![p_{\Gamma,h}]\!] \cdot [\![q_\Gamma]\!], \\ F_\Gamma(\mathbf{v}_\Gamma) &= \int_{\mathcal{E}^D_{h,\Gamma}} g_\Gamma \mathbf{v}_\Gamma \cdot \mathbf{n}_e, \\ G_\Gamma(q_\Gamma) &= \int_{\Gamma_h} f_\Gamma q_\Gamma + \int_{\mathcal{E}_{\Gamma,h}} \sigma_e g_\Gamma q_\Gamma, \end{aligned}$$

and $\mathcal{A}_b^P(p_h, q)$ and $\mathcal{L}_b^P(q)$ are defined as in (24) and (27), respectively.

Aiming at rewriting the problem in the fracture in primal form, we introduce the lifting operator, $\mathscr{L}_\Gamma^{LDG} : [L^1(\mathcal{E}_h^I \cup \mathcal{E}_h^D)]^d \to \mathbf{W}_h^\Gamma$, defined by

$$\int_{\Gamma_h} \mathscr{L}_\Gamma^{LDG}(\boldsymbol{\xi}_\Gamma) \cdot \mathbf{v}_\Gamma = -\int_{\mathcal{E}^I_{\Gamma,h}} (\{\mathbf{v}_\Gamma\} - \mathbf{b}_\Gamma [\![\mathbf{v}_\Gamma]\!]) \cdot \boldsymbol{\xi}_\Gamma - \int_{\mathcal{E}^D_{\Gamma,h}} \boldsymbol{\xi}_\Gamma \cdot \mathbf{v}_\Gamma \quad \forall\, \mathbf{v}_\Gamma \in \mathbf{W}_h^\Gamma \quad (41)$$

From equation (38) we obtain

$$\mathbf{u}_{\Gamma,h} = \boldsymbol{\nu}_\Gamma^\tau \ell_\Gamma [\nabla p_{\Gamma,h} + \mathscr{L}_\Gamma^{LDG}([\![p_{\Gamma,h}]\!]) + \mathcal{G}_\Gamma] \tag{42}$$

where $\mathcal{G}_\Gamma$ is the lifting of the Dirichlet boundary datum defined in (21). Equation (39) now becomes

$$\int_{\Gamma_h} \boldsymbol{\nu}_\Gamma^\tau \ell_\Gamma (\nabla p_{\Gamma,h} + \mathscr{L}_\Gamma^{LDG}([\![p_{\Gamma,h}]\!])) \cdot (\nabla q_\Gamma + \mathscr{L}_\Gamma^{LDG}([\![q_\Gamma]\!])) + \int_{\mathcal{E}_{\Gamma,h}^I \cup \mathcal{E}_{\Gamma,h}^D} \sigma_e [\![p_{\Gamma,h}]\!] \cdot [\![q_\Gamma]\!]$$
$$+ \int_{\Gamma_h} \alpha_\Gamma (p_{\Gamma,h}) - \{p_h\}) = \int_{\Gamma_h} f_\Gamma q_\Gamma + \int_{\mathcal{E}_{\Gamma,h}^D} \sigma_e q_\Gamma g_\Gamma - \int_{\Gamma_h} \boldsymbol{\nu}_\Gamma^\tau \ell_\Gamma \mathcal{G}_\Gamma \cdot (\nabla q_\Gamma + \mathscr{L}_\Gamma^{LDG}([\![q_\Gamma]\!])).$$

We obtain the following primal formulation: Find $(p_h, p_h^\Gamma) \in Q_h^b \times Q_h^\Gamma$ such that

$$\mathcal{A}_h^{PM}\left((p_h, p_h^\Gamma), (q, q_\Gamma)\right) = \mathcal{L}_h^{PM}(q, q_\Gamma) \quad \forall (q, q_\Gamma) \in Q_h^b \times Q_h^\Gamma, \tag{43}$$

where PM stands for *primal-mixed* and where $\mathcal{A}_h^{PM} : (Q_h^b \times Q_h^\Gamma) \times (Q_h^b \times Q_h^\Gamma) \to \mathbb{R}$ is defined as

$$\mathcal{A}_h^{PM}\left((p_h, p_h^\Gamma), (q, q_\Gamma)\right) = \mathcal{A}_b^P(p_h, q) + \mathcal{A}_\Gamma^M(p_{\Gamma,h}, q_\Gamma) + \mathcal{I}((p_h, p_{\Gamma,h}), (q, q_\Gamma)),$$

and $\mathcal{L}_h^{PM} : Q_h^b \times Q_h^\Gamma \to \mathbb{R}$ is defined as

$$\mathcal{L}_h^{PM}(q, q_\Gamma) = \mathcal{L}_b^P(q) + \mathcal{L}_\Gamma^M(q_\Gamma)$$

with

$$\begin{aligned} \mathcal{A}_\Gamma^M(p_{\Gamma,h}, q_\Gamma) = &\int_{\Gamma_h} \boldsymbol{\nu}_\Gamma^\tau \ell_\Gamma (\nabla p_{\Gamma,h} + \mathscr{L}_\Gamma^{LDG}([\![p_{\Gamma,h}]\!])) \cdot (\nabla q_\Gamma + \mathscr{L}_\Gamma^{LDG}([\![q_\Gamma]\!])) \\ &+ \int_{\mathcal{E}_{\Gamma,h}^I \cup \mathcal{E}_{\Gamma,h}^D} \sigma_e [\![p_{\Gamma,h}]\!] \cdot [\![q_\Gamma]\!], \\ \mathcal{L}_\Gamma^M(q_\Gamma) = &\int_{\Gamma_h} f_\Gamma q_\Gamma + \int_{\mathcal{E}_{\Gamma,h}^D} \sigma_e q_\Gamma g_\Gamma - \int_{\Gamma_h} \boldsymbol{\nu}_\Gamma^\tau \ell_\Gamma \mathcal{G}_\Gamma \cdot (\nabla q_\Gamma + \mathscr{L}_\Gamma^{LDG}([\![q_\Gamma]\!])). \end{aligned} \tag{44}$$

Mixed-Mixed formulation

Finally, if we approximate both the problem in the bulk and in the fracture with the LDG method, we obtain the following formulation: Find $(p_h, p_{\Gamma,h}) \in Q_h^b \times Q_h^\Gamma$ and $(\mathbf{u}_h, \mathbf{u}_{\Gamma,h}) \in \mathbf{W}_h^b \times \mathbf{W}_h^\Gamma$ such that

$$\begin{aligned} \mathcal{M}_b(\mathbf{u}_h, \mathbf{v}) + \mathcal{B}_b(p_h, \mathbf{v}) &= F_b(\mathbf{v}) \quad && \forall \mathbf{v} \in \mathbf{W}_h^b, \\ -\mathcal{B}_b(q, \mathbf{u}_h) + \mathcal{S}_b(p_h, q) + \mathcal{I}_1(p_h, q, p_{\Gamma,h}) &= G_b(q) \quad && \forall q \in Q_h^b, \\ \mathcal{M}_\Gamma(\mathbf{u}_{\Gamma,h}, \mathbf{v}_\Gamma) + \mathcal{B}_\Gamma(p_{\Gamma,h}, \mathbf{v}_\Gamma) &= F_\Gamma(\mathbf{v}_\Gamma) \quad && \forall \mathbf{v}_\Gamma \in \mathbf{W}_h^\Gamma, \\ -\mathcal{B}_\Gamma(q_\Gamma, \mathbf{u}_{\Gamma,h}) + \mathcal{S}_\Gamma(p_{\Gamma,h}, q_\Gamma) + \mathcal{I}_2(p_h, (p_{\Gamma,h}, q_\Gamma)) &= G_\Gamma(q_\Gamma) \quad && \forall q_\Gamma \in Q_h^\Gamma, \end{aligned} \tag{45}$$

This formulation, together with the definition of the lifting operators (33) and (41) and of the discrete gradients (34) and (42) is equivalent to the following: Find $(p_h, p_{\Gamma,h}) \in Q_h^b \times Q_h^\Gamma$ such that

$$\mathcal{A}_h^{MM}\left((p_h, p_h^\Gamma), (q, q_\Gamma)\right) = \mathcal{L}_h^{MM}(q, q_\Gamma) \quad \forall (q, q_\Gamma) \in Q_h^b \times Q_h^\Gamma, \tag{46}$$

where MM stands for *mixed-mixed* and where $\mathcal{A}_h^{MM} : (Q_h^b \times Q_h^\Gamma) \times (Q_h^b \times Q_h^\Gamma) \to \mathbb{R}$ is defined as

$$\mathcal{A}_h^{MM}\left((p_h, p_h^\Gamma), (q, q_\Gamma)\right) = \mathcal{A}_b^M(p_h, q) + \mathcal{A}_\Gamma^M(p_{\Gamma,h}, q_\Gamma) + \mathcal{I}((p_h, p_{\Gamma,h}), (q, q_\Gamma)),$$

and $\mathcal{L}_h^{MM} : Q_h^b \times Q_h^\Gamma \to \mathbb{R}$ is defined as

$$\mathcal{L}_h^{MM}(q, q_\Gamma) = \mathcal{L}_b^M(q) + \mathcal{L}_\Gamma^M(q_\Gamma).$$

Next, we perform a unified analysis of all of the derived DG discretizations for the fully-coupled bulk-fracture problem. We remark that the analysis will be performed considering the mixed LDG discretizations recast in their primal form, following [63]. For clarity, in Table 1 we summarize the bilinear forms for all the four approaches.

Method	Primal bilinear form
Primal-Primal (PP)	$\mathcal{A}_b^P(p, q) + \mathcal{A}_\Gamma^P(p_\Gamma, q_\Gamma) + \mathcal{I}((p, q), (p_\Gamma, q_\Gamma))$
Mixed-Primal (MP)	$\mathcal{A}_b^M(p, q) + \mathcal{A}_\Gamma^P(p_\Gamma, q_\Gamma) + \mathcal{I}((p, q), (p_\Gamma, q_\Gamma))$
Primal-Mixed (PM)	$\mathcal{A}_b^P(p, q) + \mathcal{A}_\Gamma^M(p_\Gamma, q_\Gamma) + \mathcal{I}((p, q), (p_\Gamma, q_\Gamma))$
Mixed-Mixed (MM)	$\mathcal{A}_b^M(p, q) + \mathcal{A}_\Gamma^M(p_\Gamma, q_\Gamma) + \mathcal{I}((p, q), (p_\Gamma, q_\Gamma))$

Table 1: Primal forms for the DG discretizations of the bulk-fracture problems.

The bulk, fracture and interface bilinear forms are defined in:

$\mathcal{A}_b^P(p, q)$: (24) $\mathcal{A}_\Gamma^P(p_\Gamma, q_\Gamma)$: (25) $\mathcal{I}((p, q), (p_\Gamma, q_\Gamma))$: (26)

$\mathcal{A}_b^M(p, q)$: (37) $\mathcal{A}_\Gamma^M(p_\Gamma, q_\Gamma)$: (44)

4 Well-posedness of the discrete formulations

In this section, we address the problem of stability. We prove that the primal-primal (PP) (23), mixed-primal (MP) (36), primal-mixed (PM) (43) and mixed-mixed (MM)(46) formulations are well-posed. We remark that all these formulations are *not* strongly consistent, due to the presence of the lifting operators. This implies that the analysis will be based on Strang's second Lemma, [66].

We recall that, for simplicity in the analysis, we are assuming the permeability tensors $\boldsymbol{\nu}$ and $\boldsymbol{\nu}_\Gamma^\tau$ to be piecewise constant. We will employ the following notation $\bar{\boldsymbol{\nu}}_E = |\sqrt{\boldsymbol{\nu}|_E}|_2^2$ and $\bar{\boldsymbol{\nu}}_F^\tau = |\sqrt{\boldsymbol{\nu}_\Gamma^\tau|_F}|_2^2$, where $|\cdot|_2$ denotes the l_2-norm.

To consider the boundedness and stability of our primal bilinear forms, we introduce the spaces $Q^b(h) = Q_h^b + \tilde{Q}^b$ and $Q^\Gamma(h) = Q_h^\Gamma + \tilde{Q}^\Gamma$ where $\tilde{Q}^b = \{q = (q_1, q_2) \in H^1(\Omega_1) \times H^1(\Omega_2)\} \cap H^2(\mathcal{T}_h)$ and $\tilde{Q}^\Gamma = H^1(\Gamma) \cap H^2(\Gamma_h)$. We remark that all the bilinear forms $\mathcal{A}_h^{**}(\cdot, \cdot)$ are also well-defined on the extended space $Q^b(h) \times Q^\Gamma(h)$. Further, we introduce the following *energy* norm on the discrete space $Q_h^b \times Q_h^\Gamma$

$$|||(q, q_\Gamma)|||^2 = ||q||_{DG}^2 + ||q_\Gamma||_{DG}^2 + ||(q, q_\Gamma)||_{\mathcal{I}}^2$$

where

$$||q||^2_{DG} = ||\boldsymbol{\nu}^{1/2}\nabla q||^2_{0,\mathcal{T}_h} + ||\sigma_F^{1/2}[\![q]\!]||^2_{0,\mathcal{F}_h^I\cup\mathcal{F}_h^D}$$
$$||q_\Gamma||^2_{DG} = ||(\boldsymbol{\nu}_{\boldsymbol{\Gamma}}^{\boldsymbol{\tau}}\ell_\Gamma)^{1/2}\nabla q_\Gamma||^2_{0,\Gamma_h} + ||\sigma_e^{1/2}[\![q_\Gamma]\!]||^2_{0,\mathcal{E}^I_{\Gamma,h}\cup\mathcal{E}^D_{\Gamma,h}}$$
$$||(q,q_\Gamma)||^2_{\mathcal{I}} = ||\beta_\Gamma^{1/2}[\![q]\!]||^2_{0,\Gamma_h} + ||\alpha_\Gamma^{1/2}(\{q\}-q_\Gamma)||^2_{0,\Gamma_h}$$

Note that $|||\cdot|||$ is also well defined on the extended space $Q^b(h)\times Q^\Gamma(h)$.

Since our discretization employ general polytopic grids, we need introduce some technical instruments to work in this framework [38, 36, 6, 35, 37]. In particular, we need trace inverse estimates to bound the norm of a polynomial on a polytope's face/edge by the norm on the element itself. To this aim, we give the following

Definition 4.1. A mesh $\mathcal{T}_h$ is said to be *polytopic-regular* if, for any $E\in\mathcal{T}_h$, there exists a set of non-overlapping (not necessarily shape-regular) d-dimensional simplices $\{S_E^i\}_{i=1}^{n_E}$ contained in E, such that $\bar F = \partial\bar E\cap\bar{S_E^i}$, for any face $F\subseteq\partial E$, and

$$h_E \lesssim \frac{d|S_E^i|}{|F|}, \qquad i=1,\dots,n_E,$$

with the hidden constant independent of the discretization parameters, the number of faces of the element n_E, and the face measure.

We remark that this definition does not give any restriction on the number of faces per element, nor on their measure relative to the diameter of the element the face belongs to.

Assumption 4.1. *We assume that $\mathcal{T}_h$ and Γ_h are polytopic-regular meshes.*

With this hypothesis, we can state the following inverse-trace estimate that is valid for polytopic elements [35, 37].

Lemma 4.2. *Let E be a polygon/polyhedron belonging to a mesh satisfying Definition 4.1 and let $v\in\mathbb{P}_{k_E}(E)$. Then, we have*

$$||v||^2_{L^2(\partial E)} \lesssim \frac{k_E^2}{h_E}||v||^2_{L^2(E)}, \tag{47}$$

where the hidden constant depends on the dimension d, but it is independent of the discretization parameters, of the number of faces of the element and of the relative size of the face compared to the diameter k_E of E.

The second fundamental tool to deal with polytopic discretizations, is an appropriate definition of the discontinuity penalization parameter, which allows for the use of elements with arbitrarily small faces. Taking as a reference [38, 36, 6, 35, 37], we give the following two definitions for the bulk and fracture penalty functions:

Definition 4.2. The discontinuity-penalization parameter $\sigma:\mathcal{F}_h\setminus\Gamma_h\to\mathbb{R}^+$ for the bulk problem is defined facewise as

$$\sigma(\mathbf{x}) = \sigma_0\begin{cases}\max_{E\in\{E^+,E^-\}}\frac{\bar{\boldsymbol{\nu}}_E k_E^2}{h_E} & \text{if } \mathbf{x}\subset F\in\mathcal{F}_h^I,\ \bar F=\partial\bar E^+\cap\partial\bar E^-,\\ \frac{\bar{\boldsymbol{\nu}}_E k_E^2}{h_E} & \text{if } \mathbf{x}\subset F\in\mathcal{F}_h^D,\ \bar F=\partial\bar E\cap\partial\bar\Omega,\end{cases} \tag{48}$$

with $\sigma_0>0$ independent of k_E, $|E|$ and $|F|$.

Definition 4.3. The discontinuity-penalization parameter $\sigma_\Gamma : \mathcal{E}_{\Gamma,h} \to \mathbb{R}^+$ for the fracture problem is defined edgewise as

$$\sigma_\Gamma(\mathbf{x}) = \sigma_{0,\Gamma} \begin{cases} \max_{F\in\{F^+,F^-\}} \frac{\bar{\boldsymbol{\nu}}_F^\tau k_F^2}{h_F} & \text{if } \mathbf{x} \subset e \in \mathcal{E}^I_{\Gamma,h},\ \bar{e} = \partial\bar{F}^+ \cap \partial\bar{F}^-, \\ \frac{\bar{\boldsymbol{\nu}}_F^\tau k_F^2}{h_F}, & \text{if } \mathbf{x} \subset e \in \mathcal{E}^D_{\Gamma,h},\ \bar{e} = \partial\bar{F} \cap \partial\bar{\Gamma}, \end{cases} \tag{49}$$

with $\sigma_{0,\Gamma} > 0$ independent of k_F, $|F|$ and $|e|$.

Now we have all the technical tools to work in a polytopic framework. Next, we will state and prove some estimates that will be instrumental for the proof of the well-posedness of our discrete formulations. We start deriving some bounds on the lifting operators, with arguments similar to those of [63, 64, 13]. Note that all the results hold true on the extended spaces $Q^b(h)$ and $Q^\Gamma(h)$.

Lemma 4.3. *Let $\mathscr{L}_b^{SIP}(\cdot)$ be the lifting operator defined in* (16)*. Then, for every $q \in Q^b(h)$ it holds*

$$||\boldsymbol{\nu}^{1/2}\mathscr{L}_b^{SIP}([\![q]\!])||_{0,\Omega} \lesssim \frac{1}{\sigma_0^{1/2}}||\sigma_F^{1/2}[\![q]\!]||_{0,\mathcal{F}_h^I\cup\mathcal{F}_h^D}. \tag{50}$$

Proof. Denoting by $\boldsymbol{\Pi}_{\mathbf{W}_h^b}$ the L^2-projection onto $\mathbf{W}_h^b$, by definition of the lifting operator $\mathscr{L}_b^{SIP}$ and Cauchy-Schwarz inequality, we have

$$\begin{aligned} ||\boldsymbol{\nu}^{1/2}\mathscr{L}_b^{SIP}([\![q]\!])||_{0,\Omega} &= \sup_{\mathbf{z}\in[L^2(\Omega)]^d} \frac{\int_\Omega \boldsymbol{\nu}^{1/2}\mathscr{L}_b^{SIP}([\![q]\!])\cdot\mathbf{z}}{||\mathbf{z}||_{0,\Omega}} \\ &= \sup_{\mathbf{z}\in[L^2(\Omega)]^d} \frac{\int_\Omega \mathscr{L}_b^{SIP}([\![q]\!])\cdot\boldsymbol{\Pi}_{\mathbf{W}_h^b}(\boldsymbol{\nu}^{1/2}\mathbf{z})}{||\mathbf{z}||_{0,\Omega}} \\ &= -\sup_{\mathbf{z}\in[L^2(\Omega)]^d} \frac{\int_{\mathcal{F}_h^I\cup\mathcal{F}_h^D} \sigma_F^{1/2}[\![q]\!]\cdot\sigma_F^{-1/2}\{\boldsymbol{\Pi}_{\mathbf{W}_h^b}(\boldsymbol{\nu}^{1/2}\mathbf{z})\}}{||\mathbf{z}||_{0,\Omega}} \\ &\le \sup_{\mathbf{z}\in[L^2(\Omega)]^d} \frac{||\sigma_F^{1/2}[\![q]\!]||_{0,\mathcal{F}_h^I\cup\mathcal{F}_h^D}||\sigma_F^{-1/2}\{\boldsymbol{\Pi}_{\mathbf{W}_h^b}(\boldsymbol{\nu}^{1/2}\mathbf{z})\}||_{0,\mathcal{F}_h^I\cup\mathcal{F}_h^D}}{||\mathbf{z}||_{0,\Omega}}. \end{aligned}$$

Using the triangular inequality, the definition of the penalization coefficient σ_F (48), the inverse inequality (47), the assumptions on the permeability tensor $\boldsymbol{\nu}$ and the continuity property of the L^2-projector we have

$$\begin{aligned} ||\sigma_F^{-1/2}\{\boldsymbol{\Pi}_{\mathbf{W}_h^b}(\boldsymbol{\nu}^{1/2}\mathbf{z})\}||^2_{0,\mathcal{F}_h^I\cup\mathcal{F}_h^D} &\lesssim \sum_{E\in\mathcal{T}_h} \frac{1}{\sigma_0}\frac{h_E}{\bar{\boldsymbol{\nu}}_E k_E^2}||\boldsymbol{\Pi}_{\mathbf{W}_h^b}(\boldsymbol{\nu}^{1/2}\mathbf{z})||^2_{0,\partial E} \\ &\lesssim \sum_{E\in\mathcal{T}_h} \frac{1}{\bar{\boldsymbol{\nu}}_E}\frac{1}{\sigma_0}||\boldsymbol{\Pi}_{\mathbf{W}_h^b}(\boldsymbol{\nu}^{1/2}\mathbf{z})||^2_{0,E} \lesssim \frac{1}{\sigma_0}\sum_{E\in\mathcal{T}_h}||z||^2_{0,E} = \frac{1}{\sigma_0}||z||^2_{0,\Omega}. \end{aligned} \tag{51}$$

This proves the desired estimate.

□

Lemma 4.4. *Let $\mathscr{L}_\Gamma^{SIP}(\cdot)$ be the lifting operator defined in* (20)*. Then, for every $q_\Gamma \in Q^\Gamma(h)$ it holds*

$$||(\boldsymbol{\nu}_\Gamma^\tau \ell_\Gamma)^{1/2} \mathscr{L}_\Gamma^{SIP}([\![q_\Gamma]\!])||_{0,\Gamma} \lesssim \frac{1}{\sigma_{0,\Gamma}^{1/2}} ||\sigma_e^{1/2}[\![q_\Gamma]\!]||_{0,\mathcal{E}_{\Gamma,h}^I \cup \mathcal{E}_{\Gamma,h}^D}.$$

Proof. Same arguments as in in the proof of Lemma 4.3. □

Lemma 4.5. *Let $\mathscr{L}_b^{LDG}(\cdot)$ be the lifting operator defined in* (33)*. Then, for every $q \in Q^b(h)$ it holds*

$$||\boldsymbol{\nu}^{1/2} \mathscr{L}_b^{LDG}([\![q]\!])||_{0,\Omega} \lesssim \frac{1+B}{\sigma_0^{1/2}} ||\sigma_F^{1/2}[\![q]\!]||_{0,\mathcal{F}_h^I \cup \mathcal{F}_h^D}. \tag{52}$$

Proof. We proceed as in the proof of Lemma 4.3. By definition of the lifting operator $\mathscr{L}_b^{LDG}$ and Cauchy-Schwarz inequality, we have

$$\begin{aligned}
||\boldsymbol{\nu}^{1/2} \mathscr{L}_b^{LDG}([\![q]\!])||_{0,\Omega} &= \sup_{\mathbf{z}\in[L^2(\Omega)]^d} \frac{\int_\Omega \boldsymbol{\nu}^{1/2} \mathscr{L}_b^{LDG}([\![q]\!]) \cdot \mathbf{z}}{||\mathbf{z}||_{0,\Omega}} \\
&= \sup_{\mathbf{z}\in[L^2(\Omega)]^d} \frac{\int_\Omega \mathscr{L}_b^{LDG}([\![q]\!]) \cdot \boldsymbol{\Pi}_{\mathbf{W}_h^b}(\boldsymbol{\nu}^{1/2}\mathbf{z})}{||\mathbf{z}||_{0,\Omega}} \\
&\leq \sup_{\mathbf{z}\in[L^2(\Omega)]^d} \frac{\left| -\int_{\mathcal{F}_h^I} \sigma_F^{1/2}[\![q]\!] \cdot \sigma_F^{-1/2}(\{\boldsymbol{\Pi}_{\mathbf{W}_h^b}(\boldsymbol{\nu}^{1/2}\mathbf{z})\} - \mathbf{b}[\![\boldsymbol{\Pi}_{\mathbf{W}_h^b}(\boldsymbol{\nu}^{1/2}\mathbf{z})]\!]) \right|}{||\mathbf{z}||_{0,\Omega}} \\
&\quad + \sup_{\mathbf{z}\in[L^2(\Omega)]^d} \frac{\left| -\int_{\mathcal{F}_h^D} \sigma_F^{1/2}[\![q]\!] \cdot \sigma_F^{-1/2}\boldsymbol{\Pi}_{\mathbf{W}_h^b}(\boldsymbol{\nu}^{1/2}\mathbf{z}) \right|}{||\mathbf{z}||_{0,\Omega}} \\
&\leq \sup_{\mathbf{z}\in[L^2(\Omega)]^d} \frac{||\sigma_F^{1/2}[\![q]\!]||_{0,\mathcal{F}_h^I\cup\mathcal{F}_h^D} ||\sigma_F^{-1/2}\{\boldsymbol{\Pi}_{\mathbf{W}_h^b}(\boldsymbol{\nu}^{1/2}\mathbf{z})\}||_{0,\mathcal{F}_h^I\cup\mathcal{F}_h^D}}{||\mathbf{z}||_{0,\Omega}} \\
&\quad + \sup_{\mathbf{z}\in[L^2(\Omega)]^d} \frac{||\sigma_F^{1/2}[\![q]\!]||_{0,\mathcal{F}_h^I} ||\sigma_F^{-1/2}\mathbf{b}[\![\boldsymbol{\Pi}_{\mathbf{W}_h^b}(\boldsymbol{\nu}^{1/2}\mathbf{z})]\!]||_{0,\mathcal{F}_h^I}}{||\mathbf{z}||_{0,\Omega}} \\
&= (a) + (b)
\end{aligned}$$

From (51) we know that $(a) \lesssim \frac{1}{\sigma_0^{1/2}} ||\sigma_F^{1/2}[\![q]\!]||_{0,\mathcal{F}_h^I\cup\mathcal{F}_h^D}$, while using similar arguments and bound (29) on $\mathbf{b}$, we can prove that

$$||\sigma_F^{-1/2}\mathbf{b}[\![\boldsymbol{\Pi}_{\mathbf{W}_h^b}(\boldsymbol{\nu}^{1/2}\mathbf{z})]\!]||_{0,\mathcal{F}_h^I}^2 \lesssim \frac{B^2}{\sigma_0} ||\mathbf{z}||_{0,\Omega}^2,$$

so that $(b) \lesssim \frac{B}{\sigma_0^{1/2}} ||\sigma_F^{1/2}[\![q]\!]||_{0,\mathcal{F}_h^I\cup\mathcal{F}_h^D}$. This concludes the proof. □

Lemma 4.6. *Let $\mathscr{L}_\Gamma^{LDG}(\cdot)$ be the lifting operator defined in* (41)*. Then, For every $q_\Gamma \in Q^\Gamma(h)$ it holds*

$$||(\boldsymbol{\nu}_\Gamma^\tau \ell_\Gamma)^{1/2} \mathscr{L}_\Gamma^{LDG}([\![q_\Gamma]\!])||_{0,\Gamma} \lesssim \frac{1+B_\Gamma}{\sigma_{0,\Gamma}^{1/2}} ||\sigma_e^{1/2}[\![q_\Gamma]\!]||_{0,\mathcal{E}_{\Gamma,h}^I \cup \mathcal{E}_{\Gamma,h}^D}.$$

Proof. Same arguments as in in the proof of Lemma 4.5. □

Using these results, we can now prove that the bilinear forms for the bulk problem $\mathcal{A}_b^P(\cdot,\cdot)$ and $\mathcal{A}_b^M(\cdot,\cdot)$ are continuous on $Q^b(h)$ and coercive on Q_h^b, as well as the fracture bilinear forms $\mathcal{A}_\Gamma^P(\cdot,\cdot)$ and $\mathcal{A}_\Gamma^M(\cdot,\cdot)$ are continuous on $Q^\Gamma(h)$ and coercive on Q_h^Γ.

Lemma 4.7. *$\mathcal{A}_b^P(\cdot,\cdot)$ is coercive on $Q_h^b \times Q_h^b$ and continuous on $Q^b(h) \times Q^b(h)$, that is*

$$\begin{aligned} &\mathcal{A}_b^P(q,q) \gtrsim ||q||_{DG}^2 && \forall q \in Q_h^b, \\ &\mathcal{A}_b^P(p,q) \lesssim ||p||_{DG}\,||q||_{DG} && \forall p,q \in Q^b(h), \end{aligned}$$

provided that σ_0 is chosen big enough.

Proof. We start with coercivity. Taking $p = q \in Q_h^b$, we have

$$\mathcal{A}_b^P(q,q) = \sum_{E\in\mathcal{T}_h}\left[||\boldsymbol{\nu}^{1/2}\nabla q||_{0,E}^2 + 2\int_E \boldsymbol{\nu}\mathscr{L}_b^{SIP}(\llbracket q\rrbracket)\cdot\nabla q\right] + \sum_{F\in\mathcal{F}_h^I\cup\mathcal{F}_h^D} ||\sigma_F^{1/2}\llbracket q\rrbracket||_{0,F}^2$$

From Young inequality we have

$$\begin{aligned} 2\int_E \boldsymbol{\nu}\mathscr{L}_b^{SIP}(\llbracket q\rrbracket)\cdot\nabla q &\geq -2||\boldsymbol{\nu}^{1/2}\mathscr{L}_b^{SIP}(\llbracket q\rrbracket)||_{0,E}||\boldsymbol{\nu}^{1/2}\nabla q||_{0,E} \\ &\geq -\varepsilon||\boldsymbol{\nu}^{1/2}\mathscr{L}_b^{SIP}(\llbracket q\rrbracket)||_{0,E}^2 - \frac{1}{\varepsilon}||\boldsymbol{\nu}^{1/2}\nabla q||_{0,E}^2, \end{aligned}$$

so that, using the bound on the lifting (50), we obtain

$$\begin{aligned} \mathcal{A}_b^P(q,q) &\geq \sum_{E\in\mathcal{T}_h}\left[(1-\varepsilon)\|\boldsymbol{\nu}^{1/2}\nabla q\|_{0,E}^2 - \frac{1}{\varepsilon}\|\boldsymbol{\nu}^{1/2}\mathscr{L}_b^{SIP}(\llbracket q\rrbracket)\|_{0,E}^2\right] \\ &\quad + \sum_{F\in\mathcal{F}_h^I\cup\mathcal{F}_h^D} ||\sigma_F^{1/2}\llbracket q\rrbracket||_{0,F}^2 \\ &\gtrsim (1-\varepsilon)\sum_{E\in\mathcal{T}_h}\|\boldsymbol{\nu}^{1/2}\nabla q\|_{0,E}^2 + \left(1-\frac{1}{\sigma_0\varepsilon}\right)\sum_{F\in\mathcal{F}_h^I\cup\mathcal{F}_h^D} ||\sigma_F^{1/2}\llbracket q\rrbracket||_{0,F}^2 \\ &\gtrsim ||q||_{DG}^2, \end{aligned}$$

for σ_0 big enough.

Continuity directly follows from Cauchy Schwarz inequality and the bound on the lifting (50). □

Lemma 4.8. *$\mathcal{A}_\Gamma^P(\cdot,\cdot)$ is coercive on $Q_h^\Gamma \times Q_h^\Gamma$ and continuous on $Q^\Gamma(h) \times Q^\Gamma(h)$, that is*

$$\begin{aligned} &\mathcal{A}_\Gamma^P(q_\Gamma,q_\Gamma) \gtrsim ||q_\Gamma||_{DG}^2 && \forall q_\Gamma \in Q_h^\Gamma, \\ &\mathcal{A}_\Gamma^P(p_\Gamma,q_\Gamma) \lesssim ||p_\Gamma||_{DG}\,||q_\Gamma||_{DG} && \forall p_\Gamma, q_\Gamma \in Q^\Gamma(h), \end{aligned}$$

provided that $\sigma_{0,\Gamma}$ is chosen big enough.

Proof. Analogous to the proof of Lemma 4.7. □

Lemma 4.9. *$\mathcal{A}_b^M(\cdot,\cdot)$ is coercive on $Q_h^b \times Q_h^b$ and continuous on $Q^b(h) \times Q^b(h)$, that is*

$$\mathcal{A}_b^M(q,q) \gtrsim ||q||_{DG}^2 \qquad \forall q \in Q_h^b,$$
$$\mathcal{A}_b^M(p,q) \lesssim ||p||_{DG}\,||q||_{DG} \qquad \forall p,q \in Q^b(h).$$

Proof. We start with coercivity. From Young's inequality and the bound on the lifting (52) we have, for every $0 < \varepsilon < 1$,

$$\begin{aligned}
\mathcal{A}_b^M(q,q) = \sum_{E\in\mathcal{T}_h} \Bigg[& ||\boldsymbol{\nu}^{1/2}\nabla q||_{0,E}^2 + ||\boldsymbol{\nu}^{1/2}\mathscr{L}_b^{LDG}(\llbracket q \rrbracket)||_{0,E}^2 \\
& + 2\int_E \boldsymbol{\nu}\mathscr{L}_b^{LDG}(\llbracket q \rrbracket)\cdot\nabla q \Bigg] + \sum_{F\in\mathcal{F}_h^I\cup\mathcal{F}_h^D} ||\sigma_F^{1/2}\llbracket q \rrbracket||_{0,F}^2 \\
\geq \sum_{E\in\mathcal{T}_h} & \left[(1-\varepsilon)\|\boldsymbol{\nu}^{1/2}\nabla q\|_{0,E}^2 + \left(1-\frac{1}{\varepsilon}\right)||\boldsymbol{\nu}^{1/2}\mathscr{L}_b^{LDG}(\llbracket q \rrbracket)||_{0,E}^2 \right] \\
& + \sum_{F\in\mathcal{F}_h^I\cup\mathcal{F}_h^D} ||\sigma_F^{1/2}\llbracket q \rrbracket||_{0,F}^2 \\
\gtrsim (1-\varepsilon) & \sum_{E\in\mathcal{T}_h} \|\boldsymbol{\nu}^{1/2}\nabla q\|_{0,E}^2 + (1+C) \sum_{F\in\mathcal{F}_h^I\cup\mathcal{F}_h^D} ||\sigma_F^{1/2}\llbracket q \rrbracket||_{0,F}^2
\end{aligned}$$

with $C = \frac{(1+B)}{\sigma_0\varepsilon}(1-\frac{1}{\varepsilon})$, so that $\mathcal{A}_b^M(\cdot,\cdot)$ is coercive for every choice of the parameters $\sigma_0 > 0$ and $B > 0$ [1]. Continuity is again a direct consequence of Cauchy Schwarz's inequality and the bound on the lifting (52). □

Lemma 4.10. *$\mathcal{A}_\Gamma^M(\cdot,\cdot)$ is coercive on $Q_h^\Gamma \times Q_h^\Gamma$ and continuous on $Q^\Gamma(h) \times Q^\Gamma(h)$, that is*

$$\mathcal{A}_\Gamma^M(q_\Gamma,q_\Gamma) \gtrsim ||q_\Gamma||_{DG}^2 \qquad \forall q_\Gamma \in Q_h^\Gamma,$$
$$\mathcal{A}_\Gamma^M(p_\Gamma,q_\Gamma) \lesssim ||p_\Gamma||_{DG}\,||q_\Gamma||_{DG} \qquad \forall p_\Gamma, q_\Gamma \in Q^\Gamma(h).$$

Proof. Analogous to the proof of Lemma 4.9. □

Employing Lemmas 4.7, 4.9, 4.8 and 4.10, we can easily prove the well-posedness of all of our discrete problems, as stated in the following stability result.

Proposition 4.11. *Let the penalization parameters σ for the problem in the bulk and in the fracture be defined as in* (48) *and* (49)*, respectively. Then, the fully-coupled discrete problems PP* (23)*, MP* (36)*, PM* (43) *and MM* (46) *are well-posed provided that σ_0 and $\sigma_{0,\Gamma}$ are chosen big enough for the primal formulations.*

Proof. In order to use Lax-Milgram Lemma, we prove that the bilinear forms $\mathcal{A}_h^{PP}(\cdot,\cdot)$, $\mathcal{A}_h^{MP}(\cdot,\cdot)$, $\mathcal{A}_h^{PM}(\cdot,\cdot)$ and $\mathcal{A}_h^{MM}(\cdot,\cdot)$ are continuous on $Q^b(h)\times Q^\Gamma(h)$ and coercive on $Q_h^b \times Q_h^\Gamma$.

[1] More in detail: we need $1 + C > 0$, with $0 < \varepsilon < 1$. We obtain $1 + (1-\frac{1}{\varepsilon})\frac{(1+B)^2}{\sigma_0} > 0$, that is $\varepsilon > \frac{1}{1+\frac{\sigma_0}{(1+B)^2}} = \tilde{C}$, being $0 < \tilde{C} < 1$ for every possible choice of $\sigma_0 > 0$ and $B > 0$.

We have, from Cauchy-Schwarz inequality

$$\begin{aligned}\mathcal{I}((q,q_\Gamma),(q,q_\Gamma)) &= ||(q,q_\Gamma)||_{\mathcal{I}}^2 \\ \mathcal{I}((q,q_\Gamma),(w,w_\Gamma)) &\leq \sum_{F\in\Gamma_h} ||\beta_\Gamma^{1/2}[\![q]\!]||_{L^2(F)}^2 ||\beta_\Gamma^{1/2}[\![w]\!]||_{L^2(F)}^2 \\ &\quad + \sum_{F\in\Gamma_h} ||\alpha_\Gamma^{1/2}(\{q\}-q_\Gamma)||_{L^2(F)}^2 ||\alpha_\Gamma^{1/2}(\{w\}-w_\Gamma)||_{L^2(F)}^2 \\ &\leq |||(q,q_\Gamma)||| \cdot |||(w,w_\Gamma)|||,\end{aligned}$$

so that coercivity and continuity are a direct consequence of the definition of the norm $|||\cdot|||$ and of Lemmas 4.7, 4.9, 4.8 and 4.10. The continuity of the linear operators $\mathcal{L}_h^{PP}(\cdot)$, $\mathcal{L}_h^{MP}(\cdot)$, $\mathcal{L}_h^{PM}(\cdot)$ and $\mathcal{L}_h^{MM}(\cdot)$ on $Q^b(h)\times Q^\Gamma(h)$ can be easily proved by using Cauchy-Schwarz's inequality, thanks to the regularity assumptions on the forcing terms f and f_Γ and on the boundary data g_D and g_Γ. □

5 Error analysis

In this section we derive error estimates for our discrete problems.

5.1 Approximation results

The tool at the base of DG-method error analysis are *hp*-interpolation estimates. Here, we summarize the results contained in [38, 36, 6, 35, 37], where standard estimates on simplices are extended to arbitrary polytopic elements.

First, we give the following definitions.

Definition 5.1. A *covering* $\mathcal{T}_\# = \{T_E\}$ related to the polytopic mesh $\mathcal{T}_h$ is a set of shape-regular d-dimensional simplices T_E, such that for each $E\in\mathcal{T}_h$, there exists a $T_E\in\mathcal{T}_\#$ such that $E\subsetneq T_E$.

Assumption 5.1. *[38, 36, 6, 35, 37] There exists a covering $\mathcal{T}_\#$ of $\mathcal{T}_h$ (see Definition 5.1) and a positive constant O_Ω, independent of the mesh parameters, such that*

$$\max_{E\in\mathcal{T}_h} card\{E'\in\mathcal{T}_h:\ E'\cap T_E\neq\emptyset,\ T_E\in\mathcal{T}_\#\ \ s.t.\ E\subset T_E\}\leq O_\Omega,$$

and $h_{T_E}\lesssim h_E$ for each pair $E\in\mathcal{T}_h$ and $T_E\in\mathcal{T}_\#$, with $E\subset T_E$.

Moreover, there exists a covering $\mathcal{F}_\#$ of Γ_h and a positive constant O_Γ, independent of the mesh parameters, such that

$$\max_{F\in\Gamma_h} card\{F'\in\Gamma_h:\ F'\cap T_F\neq\emptyset,\ T_F\in\mathcal{F}_\#\ \ s.t.\ F\subset T_F\}\leq O_\Gamma,$$

and $h_{T_F}\lesssim h_F$ for each pair $F\in\Gamma_h$ and $T_F\in\mathcal{F}_\#$, with $F\subset T_F$.

We can now state the following approximation result:

Lemma 5.2. [38, 36, 6, 35, 37] *Let $E \in \mathcal{T}_h$ and $T_E \in \mathcal{T}_\#$ denote the corresponding simplex such that $E \subset T_E$ (see Definition 5.1). Suppose that $v \in L^2(\Omega)$ is such that $\mathscr{E}v|_{T_E} \in H^{r_E}(T_E)$, for some $r_E \geq 0$. Then, if Assumption 4.1 and 5.1 are satisfied, there exists $\widetilde{\Pi}v$, such that $\widetilde{\Pi}v|_E \in \mathbb{P}_{k_E}(E)$, and the following bound holds*

$$||v - \widetilde{\Pi}v||_{H^q(E)} \lesssim \frac{h_E^{s_E - q}}{k_E^{r_E - q}} ||\mathscr{E}v||_{H^{r_E}(T_E)}, \qquad 0 \leq q \leq r_E. \tag{53}$$

Moreover, if $r_E > 1/2$,

$$||v - \widetilde{\Pi}v||_{L^2(\partial E)} \lesssim \frac{h_E^{s_E - 1/2}}{k_E^{r_E - 1/2}} ||\mathscr{E}v||_{H^{r_E}(T_E)}. \tag{54}$$

Here, $s_E = \min(k_E + 1, r_E)$ and the hidden constants depend on the shape-regularity of T_E, but are independent of v, h_E, k_E and the number of faces per element and $\mathscr{E}$ is the continuous extension operator as defined in [65].

Proof. See [38] for a detailed proof of (53) and [35] for the proof of (54). □

Clearly, analogous approximation results can be stated on the fracture spaces, since Assumptions 4.1 and 5.1 are both satisfied.

5.2 Error estimates

For each subdomain Ω_i, $i = 1, 2$, we denote by $\mathscr{E}_i$ the classical continuous extension operator (cf. [65], see also [9]) $\mathscr{E}_i : H^s(\Omega_i) \to H^s(\mathbb{R}^d)$, for $s \in \mathbb{N}_0$. Similarly, we denote by $\mathscr{E}_\Gamma$ the continuous extension operator $\mathscr{E}_\Gamma : H^s(\Gamma) \to H^s(\mathbb{R}^{d-1})$, for $s \in \mathbb{N}_0$. We then make the following regularity assumptions for the exact solution (p, p_Γ) of problem (7):

Assumption 5.3. *Let $\mathcal{T}_\# = \{T_E\}$ and $\mathcal{F}_\# = \{T_F\}$ denote the associated coverings of Ω and Γ, respectively, of Definition 5.1. We assume that the exact solution (p, p_Γ) is such that:*

A1. for every $E \in \mathcal{T}_h$, if $E \subset \Omega_i$, it holds $\mathscr{E}_i p_i|_{T_E} \in H^{r_E}(T_E)$, with $r_E \geq 1 + d/2$ and $T_E \in \mathcal{T}_\#$ with $E \subset T_E$;

A2. for every $F \in \Gamma_h$, it holds $\mathscr{E}_\Gamma p_\Gamma|_{T_F} \in H^{r_F}(T_F)$, with $r_F \geq 1 + (d-1)/2$ and $T_F \in \mathcal{F}_\#$ with $F \subset T_F$.

Assumption 5.4. *We assume that the normal components of the exact fluxes $\boldsymbol{\nu}\nabla p$ and $\ell_\Gamma \boldsymbol{\nu}_\Gamma^\tau \nabla p_\Gamma$ are continuous across mesh interfaces, that is $[\![\boldsymbol{\nu}\nabla p]\!] = 0$ on $\mathcal{F}_h^I$ and $[\![\ell_\Gamma \boldsymbol{\nu}_\Gamma^\tau \nabla p_\Gamma]\!] = 0$ on $\mathcal{E}_{\Gamma,h}^I$.*

From Proposition 4.11 and Strang's second Lemma the following abstract error bound directly follows.

Lemma 5.5. *Assuming that the hypotheses of Proposition 4.11 are satisfied, for all the discrete problems PP (23), MP (36), MM (46) and PM (46) the following abstract error bound holds*

$$|||(p, p_\Gamma) - (p_h, p_{\Gamma,h})||| \lesssim \inf_{(q,q_\Gamma) \in Q_h^b \times Q_h^\Gamma} |||(p, p_\Gamma) - (q, q_\Gamma)||| \quad + \sup_{(w,w_\Gamma) \in Q_h^b \times Q_h^\Gamma} \frac{|\mathcal{R}_h^{**}((p, p_\Gamma), (w, w_\Gamma))|}{|||(w, w_\Gamma)|||},$$

where the residual $\mathcal{R}_h^{**}$ *is defined as*

$$\mathcal{R}_h^{**}((p,p_\Gamma),(w,w_\Gamma)) = \mathcal{A}_h^{**}((p,p_\Gamma),(w,w_\Gamma)) - \mathcal{L}_h^{**}(w,w_\Gamma),$$

with $** \in \{PP, MP, MM, PM\}$.

Note that, irrespective of the numerical method chosen for the discretization (PP, MP, PM or MM), the residual can always be split into two contributions, one deriving from the approximation of the problem in the bulk and one deriving from the approximation of the problem in the fracture, i.e.,

$$\mathcal{R}_h^{**}((p,p_\Gamma),(w,w_\Gamma)) = \mathcal{R}_b^{*}(p,w) + \mathcal{R}_\Gamma^{*}(p_\Gamma,w_\Gamma) \tag{55}$$

It follows that, to derive a bound for the global residual, we can bound each of the two contributions separately. With this in mind, we state and prove the next two lemmas.

Lemma 5.6. *Let* (p,p_Γ) *be the exact solution of problem* (7) *satisfying the regularity Assumptions 5.4 and 5.3. Then, for every* $w \in Q^b(h)$ *and* $w_\Gamma \in Q^\Gamma(h)$*, it holds*

$$|\mathcal{R}_b^P(p,w)|^2 \lesssim \sum_{E\in\mathcal{T}_h} \frac{h_E^{2(s_E-1)}}{k_E^{2(r_E-1)}} ||\mathscr{E}p||^2_{H^{r_E}(T_E)} \Big[\bar{\boldsymbol{\nu}}_E^2 \max_{F\subset\partial E\setminus\Gamma} \sigma_F^{-1}\big(\frac{k_E}{h_E}+\frac{k_E^2}{h_E}\big)\Big] \cdot ||w||^2_{DG}, \tag{56}$$

$$|\mathcal{R}_\Gamma^P(p_\Gamma,w_\Gamma)|^2 \lesssim \sum_{F\in\Gamma_h} \frac{h_F^{2(s_F-1)}}{k_F^{2(r_F-1)}} ||\mathscr{E}p_\Gamma||^2_{H^{R_F}(T_F)} \Big[(\bar{\boldsymbol{\nu}}_F^\tau \ell_\Gamma)^2 \max_{e\subseteq\partial F} \sigma_e^{-1}\big(\frac{k_F}{h_F}+\frac{k_F^2}{h_F}\big)\Big] \cdot ||w_\Gamma||^2_{DG} \tag{57}$$

Proof. First, we prove (56). Let $\mathbf{\Pi}_{\mathbf{W}_h^b}$ be the L^2-orthogonal projector onto $\mathbf{W}_h^b$, then, integrating by parts elementwise, using the fact that p satisfies (2) and recalling that, from Assumption 5.4, $[\![\boldsymbol{\nu}\nabla p]\!]$ vanishes on $\mathcal{F}_h^I$, we obtain the following expression for the residual $\mathcal{R}_b^P$:

$$\mathcal{R}_b^P(p,w) = \sum_{F\in\mathcal{F}_h^I\cup\mathcal{F}_h^D} \int_F \{\boldsymbol{\nu}(\nabla p - \mathbf{\Pi}_{\mathbf{W}_h^b}(\nabla p))\}\cdot[\![w]\!], \qquad \forall w\in Q^b(h).$$

Employing the Cauchy-Schwarz's inequality and the definition of the norm $|||\cdot|||$, we then obtain

$$|\mathcal{R}_b^P(p,w)|^2 \lesssim \left(\sum_{F\in\mathcal{F}_h^I\cup\mathcal{F}_h^D} \sigma_F^{-1}\int_F |\{\boldsymbol{\nu}(\nabla p - \mathbf{\Pi}_{\mathbf{W}_h^b}(\nabla p))\}|^2\right)\cdot ||w||^2_{DG}, \qquad \forall w\in Q^b(h).$$

If we still denote by $\widetilde{\Pi}$ the vector-valued generalization of the projection operator $\widetilde{\Pi}$ defined in Lemma 5.2, we observe that

$$\begin{aligned}\sum_{F\in\mathcal{F}_h^I\cup\mathcal{F}_h^D} \sigma_F^{-1}\int_F |\{\boldsymbol{\nu}(\nabla p - \mathbf{\Pi}_{\mathbf{W}_h^b}(\nabla p))\}|^2 \le & \sum_{F\in\mathcal{F}_h^I\cup\mathcal{F}_h^D} \sigma_F^{-1}\int_F |\{\boldsymbol{\nu}(\nabla p - \widetilde{\Pi}(\nabla p))\}|^2 \\ & + \sum_{F\in\mathcal{F}_h^I\cup\mathcal{F}_h^D} \sigma_F^{-1}\int_F |\{\boldsymbol{\nu}\mathbf{\Pi}_{\mathbf{W}_h^b}(\nabla p - \widetilde{\Pi}(\nabla p))\}|^2 \\ & \equiv (1)+(2).\end{aligned}$$

To bound the term (1), we employ the approximation result stated in Lemma 5.2. We obtain

$$(1) \lesssim \sum_{E\in\mathcal{T}_h} \frac{h_E^{2(s_E-1)}}{k_E^{2(r_E-1)}} \big(\bar{\boldsymbol{\nu}}_E^2 \max_{F\subset\partial E\setminus\Gamma} \sigma_F^{-1} \frac{h_E^{-1}}{k_E^{-1}}\big) ||\mathscr{E}p||^2_{H^{r_E}(T_E)}.$$

Exploiting, the boundedness of the permeability tensor $\boldsymbol{\nu}$, the inverse inequality (47), the L^2-stability of the projector $\boldsymbol{\Pi}_{\mathbf{W}_h^b}$ and the approximation results stated in Lemma 5.2, we can bound term (2) as follows:

$$\begin{aligned}
(2) &\lesssim \sum_{E\in\mathcal{T}_h} \max_{F\subset\partial E\setminus\Gamma} \sigma_F^{-1} \bar{\boldsymbol{\nu}}_E^2 ||\boldsymbol{\Pi}_{\mathbf{W}_h^b}(\widetilde{\Pi}(\nabla p) - \nabla p)||^2_{L^2(\partial E\setminus\Gamma)} \\
&\lesssim \sum_{E\in\mathcal{T}_h} \max_{F\subset\partial E\setminus\Gamma} \sigma_F^{-1} \bar{\boldsymbol{\nu}}_E^2 \frac{k_E^2}{h_E} ||\widetilde{\Pi}(\nabla p) - \nabla p||^2_{L^2(E)} \\
&\lesssim \sum_{E\in\mathcal{T}_h} \frac{h_E^{2(s_E-1)}}{k_E^{2(r_E-1)}} ||\mathscr{E}p||^2_{H^{r_E}(T_E)} \Big(\bar{\boldsymbol{\nu}}_E^2 \frac{k_E^2}{h_E} \max_{F\subset\partial E\setminus\Gamma} \sigma_F^{-1}\Big),
\end{aligned}$$

which concludes the proof of (56).
Proceeding as above we obtain the following expression for the residual $\mathcal{R}_\Gamma^P$:

$$\mathcal{R}_\Gamma^P(p_\Gamma, w_\Gamma) = \sum_{e\in\mathcal{E}_{\Gamma,h}^I\cup\mathcal{E}_{\Gamma,h}^D} \int_e \{\boldsymbol{\nu}_{\boldsymbol{\Gamma}}^{\boldsymbol{\tau}} \ell_\Gamma(\nabla p_\Gamma - \boldsymbol{\Pi}_{\mathbf{W}_h^\Gamma}(\nabla p_\Gamma))\} \cdot [\![w_\Gamma]\!].$$

Estimate (57) can then be proven with analogous arguments. □

Lemma 5.7. *Let (p, p_Γ) be the exact solution of problem (7) satisfying the regularity Assumptions 5.4 and 5.3. Then, for every $w \in Q^b(h)$ and $w_\Gamma \in Q^\Gamma(h)$, it holds*

$$|\mathcal{R}_b^M(p,w)|^2 \lesssim \sum_{E\in\mathcal{T}_h} \frac{h_E^{2(s_E-1)}}{k_E^{2(r_E-1)}} ||\mathscr{E}p||^2_{H^{r_E}(T_E)} \Big[(1+B)\bar{\boldsymbol{\nu}}_E^2 \max_{F\subset\partial E\setminus\Gamma} \sigma_F^{-1}(\frac{k_E}{h_E} + \frac{k_E^2}{h_E})\Big] \cdot ||w||^2_{DG}, \tag{58}$$

$$|\mathcal{R}_\Gamma^M(p_\Gamma, w_\Gamma)|^2 \lesssim \sum_{F\in\Gamma_h} \frac{h_F^{2(s_F-1)}}{k_F^{2(r_F-1)}} ||\mathscr{E}p_\Gamma||^2_{H^{R_F}(T_F)} \Big[(1+B_\Gamma)(\bar{\boldsymbol{\nu}}_F^\tau \ell_\Gamma)^2 \max_{e\subseteq\partial F} \sigma_e^{-1}(\frac{k_F}{h_F} + \frac{k_F^2}{h_F})\Big] \cdot ||w_\Gamma||^2_{DG}. \tag{59}$$

Proof. We focus on the proof of (58), estimate (59) can be obtained likewise. Recalling that $\boldsymbol{\Pi}_{\mathbf{W}_h^b}$ denotes the L^2-orthogonal projector onto $\mathbf{W}_h^b$, the residual $\mathcal{R}_b^M$ has the following expression:

$$\begin{aligned}
\mathcal{R}_b^M(p,w) = &\sum_{F\in\mathcal{F}_h^I\cup\mathcal{F}_h^D} \int_F \Big(\{\boldsymbol{\nu}(\nabla p - \boldsymbol{\Pi}_{\mathbf{W}_h^b}(\nabla p))\} - \mathbf{b}[\![\boldsymbol{\nu}(\nabla p - \boldsymbol{\Pi}_{\mathbf{W}_h^b}(\nabla p))]\!]\Big) \cdot [\![w]\!] \\
&+ \sum_{F\in\mathcal{F}_h^D} \int_F w\boldsymbol{\nu}(\nabla p - \boldsymbol{\Pi}_{\mathbf{W}_h^b}(\nabla p)) \cdot \mathbf{n}_F,
\end{aligned}$$

where we have used the identity $\mathscr{L}_b^{LDG}([\![p]\!]) = -\mathcal{G}_b$ and the continuity of $\boldsymbol{\nu}\nabla p$ across internal faces (Assumption 5.4). From Cauchy-Schwarz and triangular inequalities and the bound on the coefficient $\mathbf{b}$ (29), we have

$$|\mathcal{R}_b^M(p,w)|^2 \lesssim \Bigg(\sum_{F\in\mathcal{F}_h^I\cup\mathcal{F}_h^D} \sigma_F^{-1}\Big[\int_F |\{\boldsymbol{\nu}(\nabla p - \widetilde{\Pi}(\nabla p))\}|^2 + \int_F |\{\boldsymbol{\nu}\boldsymbol{\Pi}_{\mathbf{W}_h^b}(\nabla p - \widetilde{\Pi}(\nabla p))\}|^2\Big]$$
$$+ B \sum_{F\in\mathcal{F}_h^I\cup\mathcal{F}_h^D} \sigma_F^{-1}\Big[\int_F |[\![\boldsymbol{\nu}(\nabla p - \widetilde{\Pi}(\nabla p))]\!]|^2 + \int_F |[\![\boldsymbol{\nu}\boldsymbol{\Pi}_{\mathbf{W}_h^b}(\nabla p - \widetilde{\Pi}(\nabla p))]\!]|^2\Big]\Bigg) \cdot ||w||_{DG}^2,$$

where we recall that, with a slight abuse of notation, $\widetilde{\Pi}$ still denotes the vector-valued generalization of the projection operator $\widetilde{\Pi}$ defined in Lemma 5.2. The thesis now follows from the boundedness of the permeability tensor $\boldsymbol{\nu}$, the inverse inequality (47), the L^2-stability of the projector $\boldsymbol{\Pi}_{\mathbf{W}_h^b}$ and the approximation results stated in Lemma 5.2.

□

Theorem 5.8. *Let $\mathcal{T}_\# = \{T_E\}$ and $\mathcal{F}_\# = \{T_F\}$ denote the associated coverings of Ω and Γ, respectively, consisting of shape-regular simplexes as in Definition 5.1, satisfying Assumptions 5.1. Let (p, p_Γ) be the solution of problem (7) and $(p_h, p_{\Gamma,h}) \in Q_h^b \times Q_h^\Gamma$ be its approximation obtained with the method PP, MP, MM or PM, with the penalization parameters given by (48) and (49) and σ_0 and $\sigma_{0,\Gamma}$ sufficiently large for the primal formulations. Moreover, suppose that the exact solution (p, p_Γ) satisfies the regularity Assumptions 5.4 and 5.3. Then, the following error bound holds:*

$$|||(p,p_\Gamma) - (p_h,p_{\Gamma,h})|||^2 \lesssim \sum_{E\in\mathcal{T}_h} \frac{h_E^{2(s_E-1)}}{k_E^{2(r_E-1)}} G_E^*(h_E,k_E,\bar{\boldsymbol{\nu}}_E)||\mathscr{E}p||^2_{H^{r_E}(T_E)}$$
$$+ \sum_{F\in\Gamma_h} \frac{h_F^{2(s_F-1)}}{k_F^{2(r_F-1)}} G_F^*(h_F,k_F,\bar{\boldsymbol{\nu}}_F^\tau)||\mathscr{E}_\Gamma p_\Gamma||^2_{H^{r_F}(T_F)},$$

where the $\mathscr{E}p$ is to be interpreted as $\mathscr{E}_1 p_1$ when $E \subset \Omega_1$ or as $\mathscr{E}_2 p_2$ when $E \subset \Omega_2$. Here, $s_E = \min(k_E+1, r_E)$ and $s_F = \min(k_F+1, r_F)$, and the constants are defined according to the chosen approximation method as follows:

$$\begin{aligned}
G_E^P(h_E,k_E,\bar{\boldsymbol{\nu}}_E) &= \bar{\boldsymbol{\nu}}_E + h_E k_E^{-1} \max_{F\subset\partial E\setminus\Gamma} \sigma_F + (\alpha_\Gamma+\beta_\Gamma) h_E k_E^{-1} \\
&\quad + \bar{\boldsymbol{\nu}}_E^2 h_E^{-1} k_E \max_{F\subset\partial E\setminus\Gamma} \sigma_F^{-1} + \bar{\boldsymbol{\nu}}_E^2 h_E^{-1} k_E^2 \max_{F\subset\partial E\setminus\Gamma} \sigma_F^{-1}, \\
G_F^P(h_F,k_F,\bar{\boldsymbol{\nu}}_F^\tau) &= \bar{\boldsymbol{\nu}}_F^\tau \ell_\Gamma + h_F k_F^{-1} \max_{e\subseteq\partial F} \sigma_e + \alpha_\Gamma h_F^2 k_F^{-2} \\
&\quad + (\bar{\boldsymbol{\nu}}_F^\tau \ell_\Gamma)^2 h_F^{-1} k_F \max_{e\subseteq\partial F} \sigma_e^{-1} + (\bar{\boldsymbol{\nu}}_F^\tau \ell_\Gamma)^2 h_F^{-1} k_F^2 \max_{e\subseteq\partial F} \sigma_e^{-1}, \\
G_E^M(h_E,k_E,\bar{\boldsymbol{\nu}}_E) &= \bar{\boldsymbol{\nu}}_E + h_E k_E^{-1} \max_{F\subset\partial E\setminus\Gamma} \sigma_F + (\alpha_\Gamma+\beta_\Gamma) h_E k_E^{-1} \\
&\quad + (1+B)\bar{\boldsymbol{\nu}}_E^2 h_E^{-1} k_E \max_{F\subset\partial E\setminus\Gamma} \sigma_F^{-1} + (1+B)\bar{\boldsymbol{\nu}}_E^2 h_E^{-1} k_E^2 \max_{F\subset\partial E\setminus\Gamma} \sigma_F^{-1}, \\
G_F^M(h_F,k_F,\bar{\boldsymbol{\nu}}_F^\tau) &= \bar{\boldsymbol{\nu}}_F^\tau \ell_\Gamma + h_F k_F^{-1} \max_{e\subseteq\partial F} \sigma_e + \alpha_\Gamma h_F^2 k_F^{-2} \\
&\quad + (1+B_\Gamma)(\bar{\boldsymbol{\nu}}_F^\tau \ell_\Gamma)^2 h_F^{-1} k_F \max_{e\subseteq\partial F} \sigma_e^{-1} + (1+B_\Gamma)(\bar{\boldsymbol{\nu}}_F^\tau \ell_\Gamma)^2 h_F^{-1} k_F^2 \max_{e\subseteq\partial F} \sigma_e^{-1}.
\end{aligned}$$

Proof. From Lemma 5.5 we know that the error satisfies the following bound

$$|||(p,p_\Gamma)-(p_h,p_{\Gamma,h})||| \lesssim \underbrace{\inf_{(q,q_\Gamma)\in Q_h^b\times Q_h^\Gamma} |||(p,p_\Gamma)-(q,q_\Gamma)|||}_{I} + \underbrace{\sup_{(w,w_\Gamma)\in Q_h^b\times Q_h^\Gamma} \frac{|\mathcal{R}_h((p,p_\Gamma),(w,w_\Gamma))|}{|||(w,w_\Gamma)|||}}_{II}. \quad (60)$$

We estimate the two terms on the right-hand side of (60) separately. We can rewrite term I as

$$\begin{aligned} I &= \inf_{(q,q_\Gamma)\in Q_h^b\times Q_h^\Gamma} \Big(||p-q||_{DG}^2+||p_\Gamma-q_\Gamma||_{DG}^2+||(p-q,p_\Gamma-q_\Gamma||_{\mathcal{I}}^2\Big) \\ &\le \underbrace{||p-\widetilde{\Pi}p||_{DG}^2}_{(a)}+\underbrace{||p_\Gamma-\widetilde{\Pi}p_\Gamma||_{DG}^2}_{(b)}+\underbrace{||(p-\widetilde{\Pi}p,p_\Gamma-\widetilde{\Pi}p_\Gamma)||_{\mathcal{I}}^2}_{(c)}. \end{aligned}$$

Again we consider each of the three terms separately. To bound term (a), we exploit the two approximation results stated in Lemma 5.2 and obtain

$$\begin{aligned} (a) &\le ||p-\widetilde{\Pi}p||_{DG}^2 = \sum_{E\in\mathcal{T}_h}||\boldsymbol{\nu}^{1/2}\nabla(p-\widetilde{\Pi}p)||_{L^2(E)}^2+\sum_{F\in\mathcal{F}_h^I\cup\mathcal{F}_h^D}\sigma_F||[\![p-\widetilde{\Pi}p]\!]||_{L^2(F)}^2 \\ &\lesssim \sum_{E\in\mathcal{T}_h}\Big[\bar{\boldsymbol{\nu}}_E|p-\widetilde{\Pi}p|_{H^1(E)}^2+(\max_{F\subset\partial E\setminus\Gamma}\sigma_F)||p-\widetilde{\Pi}p||_{L^2(\partial E\setminus\Gamma)}^2\Big] \\ &\lesssim \sum_{E\in\mathcal{T}_h}\Big[\frac{h_E^{2(s_E-1)}}{k_E^{2(r_E-1)}}\bar{\boldsymbol{\nu}}_E||\mathscr{E}p||_{H^{r_E}(T_E)}^2+\sum_{F\subset\partial E\setminus\Gamma}\frac{h_E^{2(s_E-1/2)}}{k_E^{2(r_E-1/2)}}(\max_{F\subset\partial E\setminus\Gamma}\sigma_F)||\mathscr{E}p||_{H^{r_E}(T_E)}^2\Big] \\ &= \sum_{E\in\mathcal{T}_h}\frac{h_E^{2(s_E-1)}}{k_E^{2(r_E-1)}}||\mathscr{E}p||_{H^{r_E}(T_E)}^2\Big(\bar{\boldsymbol{\nu}}_E+\frac{h_E}{k_E}(\max_{F\subset\partial E\setminus\Gamma}\sigma_F)\Big). \end{aligned}$$

Using analogous interpolation estimates on the fracture we can bound term (b) as follows:

$$\begin{aligned} (b) &\le ||p_\Gamma-\widetilde{\Pi}p_\Gamma||_{DG}^2 \lesssim \sum_{F\in\Gamma_h}||\boldsymbol{\nu}_\Gamma^\tau\ell_\Gamma\nabla(p_\Gamma-\widetilde{\Pi}p_\Gamma)||_{L^2(F)}^2+\sum_{e\in\mathcal{E}_{\Gamma,h}^I\cup\mathcal{E}_{\Gamma,h}^D}\sigma_e||[\![p_\Gamma-\widetilde{\Pi}p_\Gamma]\!]||_{L^2(e)}^2 \\ &\lesssim \sum_{F\in\Gamma_h}\frac{h_F^{2(s_F-1)}}{k_F^{2(r_F-1)}}||\mathscr{E}p_\Gamma||_{H^{R_F}(T_F)}^2\left(\bar{\boldsymbol{\nu}}_F^\tau\ell_\Gamma+\frac{h_F}{k_F}\max_{e\subseteq\partial F}\sigma_e\right) \end{aligned}$$

Finally, for term (c), we have

$$\begin{aligned} (c) \le ||(p-\widetilde{\Pi}p,p_\Gamma-\widetilde{\Pi}p_\Gamma)||_{\mathcal{I}}^2 \le \beta_\Gamma\sum_{F\in\Gamma_h}||[\![p-\widetilde{\Pi}p]\!]||_{L^2(F)}^2+\alpha_\Gamma\sum_{F\in\Gamma_h}||\{p-\widetilde{\Pi}p\}||_{L^2(F)}^2 \\ +\alpha_\Gamma\sum_{F\in\Gamma_h}||p_\Gamma-\widetilde{\Pi}p_\Gamma||_{L^2(F)}^2. \end{aligned}$$

Exploiting the approximation result (54), we obtain

$$\beta_\Gamma \sum_{F\in\Gamma_h} |||[\![p-\widetilde{\Pi}p]\!]||^2_{L^2(F)} \le \beta_\Gamma \sum_{\substack{E\in\mathcal{T}_h\\ \partial E\cap\Gamma\neq\emptyset}} ||p-\widetilde{\Pi}p||^2_{L^2(\partial E)} \lesssim \beta_\Gamma \sum_{\substack{E\in\mathcal{T}_h\\ \partial E\cap\Gamma\neq\emptyset}} \frac{h_E^{2(s_E-\frac{1}{2})}}{k_E^{2(r_E-\frac{1}{2})}} ||\mathscr{E}p||^2_{H^{r_E}(T_E)}$$
$$= \beta_\Gamma \sum_{\substack{E\in\mathcal{T}_h\\ \partial E\cap\Gamma\neq\emptyset}} \frac{h_E^{2(s_E-1)}}{k_E^{2(r_E-1)}} ||\mathscr{E}p||^2_{H^{r_E}(T_E)} \frac{h_E}{k_E}.$$

Similarly, we have

$$\alpha_\Gamma \sum_{F\in\Gamma_h} ||\{p-\widetilde{\Pi}p\}||^2_{L^2(F)} \lesssim \alpha_\Gamma \sum_{\substack{E\in\mathcal{T}_h\\ \partial E\cap\Gamma\neq\emptyset}} \frac{h_E^{2(s_E-1)}}{k_E^{2(r_E-1)}} ||\mathscr{E}p||^2_{H^{r_E}(T_E)} \frac{h_E}{k_E}.$$

Finally, using the interpolation estimates for the fracture, we deduce that

$$\alpha_\Gamma \sum_{F\in\Gamma_h} ||p_\Gamma-\widetilde{\Pi}p_\Gamma||^2_{L^2(F)} \lesssim \alpha_\Gamma \sum_{F\in\Gamma_h} \frac{h_F^{2s_F}}{k^{2r_F}} ||\mathscr{E}p_\Gamma||^2_{H^{r_F}(T_F)}$$
$$= \alpha_\Gamma \sum_{F\in\Gamma_h} \frac{h_F^{2(s_F-1)}}{k_F^{2(r_F-1)}} ||\mathscr{E}p_\Gamma||^2_{H^{R_F}(T_F)} \frac{h_F^2}{k_F^2}.$$

In conclusion, combining all the previous estimates, we can bound the term I on the right-hand side of (60) as follows:

$$I \lesssim \frac{h_E^{2(s_E-1)}}{k_E^{2(r_E-1)}} ||\mathscr{E}p||^2_{H^{r_E}(T_E)} \Big[\bar{\boldsymbol{\nu}}_E + \frac{h_E}{k_E} \max_{F\subset\partial E\setminus\Gamma} \sigma_F + (\alpha_\Gamma+\beta_\Gamma)\frac{h_E}{k_E}\Big]$$
$$+ \sum_{F\in\Gamma_h} \frac{h_F^{2(s_F-1)}}{k_F^{2(r_F-1)}} ||\mathscr{E}p_\Gamma||^2_{H^{R_F}(T_F)} \left[\bar{\boldsymbol{\nu}}_F^\tau \ell_\Gamma + \frac{h_F}{k_F} \max_{e\subseteq\partial F} \sigma_e + \alpha_\Gamma \frac{h_F^2}{k_F^2}\right]. \quad (61)$$

Finally, the desired estimates follow from the combination of (61), together with the bound on Term II deriving from what observed in (55) and Lemmas 5.6 and 5.7. □

Finally, from the above result we can derive some error estimates also for the velocities $\mathbf{u}$ and $\mathbf{u}_\Gamma$.

Theorem 5.9. *Let all the hypotheses of Theorem 5.8 hold. Let* $(\boldsymbol{u},\boldsymbol{u}_\Gamma)\in \boldsymbol{W}_g$ *and* $(p,p_\Gamma)\in M$ *be the solution of problem* (7)*. Then:*

- *if* $\big((p_h,\boldsymbol{u}_h),p_{\Gamma,h}\big)\in Q_h^b\times\boldsymbol{W}_h^b\times Q_h^\Gamma$ *is its approximation obtained with the MP method* (32)*, it holds*

$$||\boldsymbol{u}-\boldsymbol{u}_h||^2_{0,\mathcal{T}_h} \lesssim \sum_{E\in\mathcal{T}_h} \frac{h_E^{2(s_E-1)}}{k_E^{2(r_E-1)}} G_E^M ||\mathscr{E}p||^2_{H^{r_E}(T_E)} + \sum_{F\in\Gamma_h} \frac{h_F^{2(s_F-1)}}{k_F^{2(r_F-1)}} G_F^P ||\mathscr{E}_\Gamma p_\Gamma||^2_{H^{r_F}(T_F)};$$

- *if* $\big(p_h, (p_{\Gamma,h}, \boldsymbol{u}_{\Gamma,h})\big) \in Q_h^b \times Q_h^\Gamma \times \boldsymbol{W}_h^\Gamma$ *is its approximation obtained with the PM method* (40)*, it holds*

$$||\boldsymbol{u}_\Gamma - \boldsymbol{u}_{\Gamma,h}||^2_{0,\Gamma_h} \lesssim \sum_{E\in\mathcal{T}_h} \frac{h_E^{2(s_E-1)}}{k_E^{2(r_E-1)}} G_E^P ||\mathscr{E}p||^2_{H^{r_E}(T_E)} + \sum_{F\in\Gamma_h} \frac{h_F^{2(s_F-1)}}{k_F^{2(r_F-1)}} G_F^M ||\mathscr{E}_\Gamma p_\Gamma||^2_{H^{r_F}(T_F)};$$

- *if* $\big((p_h, \boldsymbol{u}_h), (p_{\Gamma,h}, \boldsymbol{u}_{\Gamma,h})\big) \in Q_h^b \times \boldsymbol{W}_h^b \times Q_h^\Gamma \times \boldsymbol{W}_h^\Gamma$ *is its approximation obtained with the MM method* (45)*, it holds*

$$\begin{aligned} ||\boldsymbol{u} - \boldsymbol{u}_h||^2_{0,\mathcal{T}_h} + ||\boldsymbol{u}_\Gamma - \boldsymbol{u}_{\Gamma,h}||^2_{0,\Gamma_h} \lesssim & \sum_{E\in\mathcal{T}_h} \frac{h_E^{2(s_E-1)}}{k_E^{2(r_E-1)}} G_E^M ||\mathscr{E}p||^2_{H^{r_E}(T_E)} \\ & + \sum_{F\in\Gamma_h} \frac{h_F^{2(s_F-1)}}{k_F^{2(r_F-1)}} G_F^M ||\mathscr{E}_\Gamma p_\Gamma||^2_{H^{r_F}(T_F)}, \end{aligned}$$

where the constants G_E^M*,* G_F^P*,* G_E^P *and* G_F^M *are defined as in Theorem 5.8.*

Proof. Let $\big((p_h, \mathbf{u}_h), p_{\Gamma,h}\big)$ and $\big((p_h, p_{\Gamma,h}), (\mathbf{u}_h, \mathbf{u}_{\Gamma,h})\big)$ be the discrete solutions obtained with the MP method and with the MM method, respectively. Then, using identity (34) and the fact that $\mathscr{L}_b^{LDG}(\llbracket p \rrbracket) = -\mathcal{G}_b$, we can rewrite

$$\begin{aligned} \mathbf{u}_h - \mathbf{u} &= \boldsymbol{\nu}\nabla p_h + \boldsymbol{\nu}\mathscr{L}_b^{LDG}(\llbracket p_h \rrbracket) + \boldsymbol{\nu}\mathcal{G}_b - \boldsymbol{\nu}\nabla p \\ &= \boldsymbol{\nu}(\nabla p_h - \nabla p) + \boldsymbol{\nu}\mathscr{L}_b^{LDG}(\llbracket p_h - p \rrbracket). \end{aligned}$$

From the uniform boundedness of $\boldsymbol{\nu}$, the triangular inequality, the bound on the lifting (52) and the definition of the $||\cdot||_{DG}$ norm it follows that

$$\begin{aligned} ||\mathbf{u} - \mathbf{u}_h||_{0,\mathcal{T}_h} &\lesssim ||\boldsymbol{\nu}^{1/2}\nabla(p_h - p)||_{0,\mathcal{T}_h} + ||\boldsymbol{\nu}^{1/2}\mathscr{L}_b^{LDG}(\llbracket p_h - p \rrbracket)||_{0,\mathcal{T}_h} \\ &\lesssim ||p_h - p||_{DG} + \frac{1+B}{\sigma_0^{1/2}} ||\sigma_F^{1/2}\llbracket p_h - p \rrbracket||_{0,\mathcal{F}_h^I\cup\mathcal{F}_h^D} \\ &\lesssim ||p_h - p||_{DG}. \end{aligned}$$

In particular, this implies that

$$||\mathbf{u} - \mathbf{u}_h||_{0,\mathcal{T}_h} \lesssim |||(p, p_\Gamma) - (p_h, p_{\Gamma,h})|||,$$

Similarly, one can prove that, if $\big(p_h, (p_{\Gamma,h}, \mathbf{u}_{\Gamma,h})\big)$ and $\big((p_h, p_{\Gamma,h}), (\mathbf{u}_h, \mathbf{u}_{\Gamma,h})\big)$ are the discrete solutions obtained with the PM method and with the MM method, respectively, it holds

$$||\mathbf{u}_\Gamma - \mathbf{u}_{\Gamma,h}||_{0,\Gamma_h} \lesssim |||(p, p_\Gamma) - (p_h, p_{\Gamma,h})|||.$$

The thesis is now a direct consequence of Theorem 5.8. □

6 Numerical experiments

In this section we present some two-dimensional numerical experiments with the aim of validating the obtained theoretical convergence results. The validity of the error estimates for the primal-primal setting has been already confirmed in [9]. Here, we focus on the paradigmatic *mixed-primal* setting. This means that, for the approximation of the problem in the bulk, we will employ the LDG method, while, for the problem in the fracture, we will employ the SIPDG method (both in their generalization to polygonal grids). All the numerical test have been implemented in MATLAB®. For the generation of polygonal meshes conforming to the fractures we have suitably modified code `PolyMesher` [69].

In particular, we present three sets of numerical experiments. The first set is obtained assuming that an analytical solution is known and aims at verifying the a-priori error estimates obtained in Theorems 5.8 and 5.9. The second set is derived form physical considerations and aims at testing how different values of the fracture permeability may influence the flow in the bulk. Finally, the last set of experiments aims at showing how the method is capable of handling more complicated geometries, specifically networks of partially immersed fractures.

6.1 Example 1: analytical solution

In this first test case we take $\Omega = (0,1)^2$, and choose as exact solutions in the bulk and in the fracture $\Gamma = \{(x,y) \in \Omega : \ x + y = 1\}$

$$p = \begin{cases} e^{x+y} & \text{in } \Omega_1, \\ e^{x+y} + \frac{4\eta_\Gamma}{\sqrt{2}} e & \text{in } \Omega_2, \end{cases} \qquad \mathbf{u} = \begin{cases} -e^{x+y} & \text{in } \Omega_1, \\ -e^{x+y} & \text{in } \Omega_2, \end{cases} \qquad p_\Gamma = e + \frac{2\eta_\Gamma}{\sqrt{2}} e.$$

It is easy to prove that $\mathbf{u}$, p and p_Γ satisfy the coupling conditions (5a)-(5b) with $\xi = 1$, $\ell_\Gamma = 0.001$ and $\boldsymbol{\nu} = \boldsymbol{\nu}_\Gamma = \mathbf{I}$. Note that in this case $f_\Gamma = 0$ since the solution in the fracture is constant and $[\![\mathbf{u}]\!] = 0$.

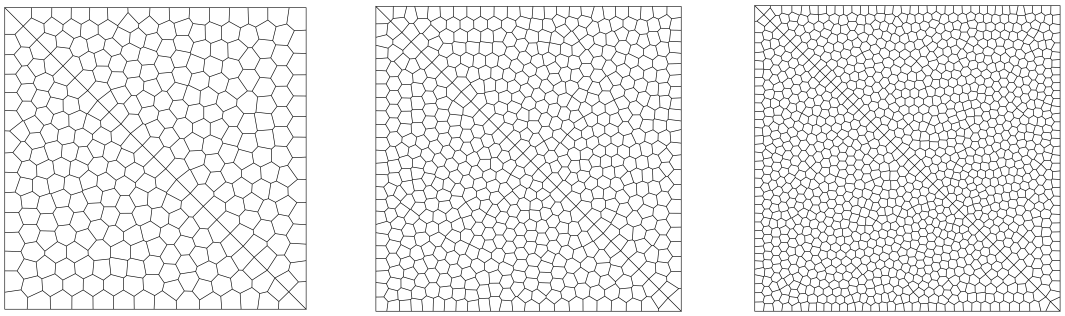

(a) (b) (c)

Figure 2: Example 1: Three refinements of the polygonal mesh grid aligned with the fracture.

Figure 2 shows three successive levels of refinements for the polygonal mesh employed in this set of experiments. In order to test the h-convergence properties of our method, we split the error in the two contributions given by the bulk and fracture errors. In particular, aiming at validating the error estimate in Theorem 5.8, we compute $||p - p_h||_{1,\Omega}$ (Figure 3(a))

and $||p^\Gamma - p_h^\Gamma||_{1,\Omega}$ (Figure 3(d)), while to validate the results of Theorem 5.9, we compute $||\mathbf{u} - \mathbf{u}_h||_{0,\Omega}$ (Figure 3(c)). In addition, we test the behaviour of the L^2-norm of the error for the primal variables, i.e., $||p - p_h||_{0,\Omega}$ (Figure 3(b)) and $||p^\Gamma - p_h^\Gamma||_{0,\Omega}$ (Figure 3(e)). All the plots in Figure 3 show the computed errors as a function of the inverse of the mesh size (loglog scale), together with the expected convergence rates. Each plot consists of four lines: every line shows the behaviour of the computed error for a different polynomial degree in the bulk (we consider $k = 1, 2, 3, 4$). For the fracture problem we always choose $k_\Gamma = 2$.

In Figures 3(a), 3(d) and 3(c) the theoretical convergence rates are clearly achieved. We observe that, in Figure 3(d), the convergence rate for $||p^\Gamma - p_h^\Gamma||_{1,\Omega}$ with $k = 1$ is suboptimal. This is due to the fact that the polynomial degree for the problem in the bulk is not accurate enough. Optimal rates are recovered for bulk polynomial degree $k = 2, 3, 4$. Finally, Figures 3(b) and 3(e) show that one order of convergence is gained for the L^2-norm for both the bulk and fracture problems.

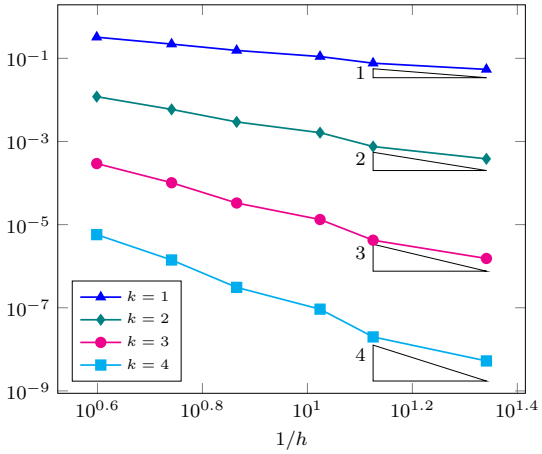

(a) $||p - p_h||_{1,\Omega}$

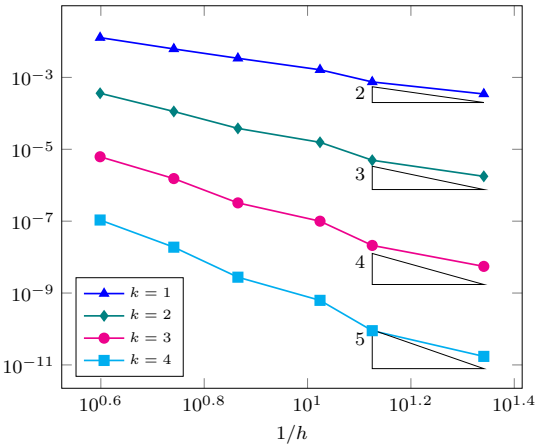

(b) $||p - p_h||_{0,\Omega}$

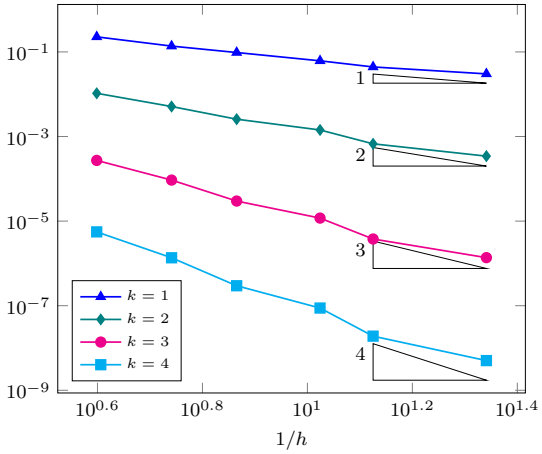

(c) $||\mathbf{u} - \mathbf{u}_h||_{0,\Omega}$

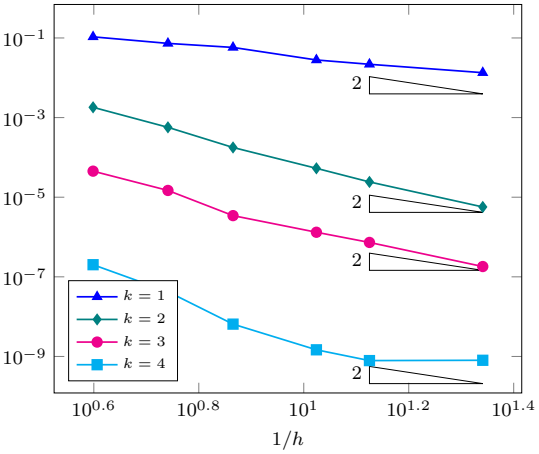

(d) $||p^\Gamma - p_h^\Gamma||_{1,\Gamma}$

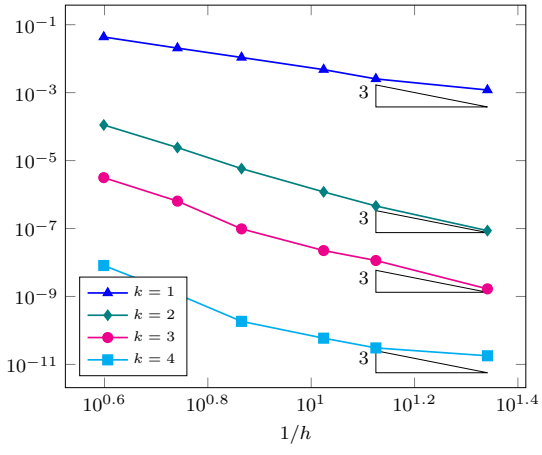

(e) $||p^\Gamma - p_h^\Gamma||_{0,\Gamma}$

Figure 3: Example 1: Computed errors as a function of $1/h$ (loglog scale) and expected convergence rates for bulk polynomial degree $k = 1, 2, 3, 4$ and fracture polynomial degree $k_\Gamma = 2$.

6.2 Example 2: discontinuous fracture permeability

Next, we reproduce some numerical experiments first presented in [62]. We examine two test cases with bulk domain $\Omega = (0,2) \times (0,1)$ and fracture domain $\Gamma = \{(x,y) \in \mathbb{R}^2 : x = 1, 0 \leq y \leq 1\}$. In the first case, we consider a fracture with constant permeability, while in the second case we consider a fracture with lower permeability in its middle part, thus presenting a discontinuity. In particular:

(a) **Case 1: constant permeability**: The permeability tensor in the fracture is given by $\boldsymbol{\nu}_\Gamma^n = \boldsymbol{\nu}_\Gamma^\tau = 100$. The bulk permeability $\boldsymbol{\nu}$ is chosen to be constant and isotropic, i.e., $\boldsymbol{\nu} = \mathbf{I}$. We impose Dirichlet boundary conditions on the left and right side of the bulk domain and homogeneous Neumann conditions on the top and bottom sides. On the fracture boundaries we impose Dirichlet boundary conditions.

(b) **Case 2: discontinous permeabilty**: The fracture Γ is subdivided into two areas having different values for the permeability tensor: in the initial and ending part of the fracture $\Gamma_1 = \{(x,y) \in \Gamma,\ 0 \leq y \leq 0.25 \text{ and } 0.75 \leq y \leq 1\}$ the permeability tensor $\boldsymbol{\nu}_{\Gamma_1}$ is defined as $\boldsymbol{\nu}_{\Gamma_1}^n = \boldsymbol{\nu}_{\Gamma_1}^\tau = 1$, while in the middle part $\Gamma_2 = \{(x,y) \in \Gamma, 0.25 \leq y \leq 0.75\}$ the permeability is low and is defined as $\boldsymbol{\nu}_{\Gamma_2}^n = \boldsymbol{\nu}_{\Gamma_2}^\tau = 0.002$. The bulk permeability tensor is chosen again equal to the identity matrix, i.e., $\boldsymbol{\nu} = \mathbf{I}$. In the bulk, we impose the same boundary conditions as in the previous test case, while at the fracture extremities we impose homogeneous Neumann conditions.

The two geometrical configurations are shown in Figures 4(a)-4(b), together with the boundary conditions. For both test cases we take the fracture thickness $\ell_\Gamma = 0.01$ and the model parameter $\xi = 2/3$. Moreover, we discretize the problem in the bulk taking as polynomial degree $k = 1$ and the problem in the fracture taking $k_\Gamma = 2$.

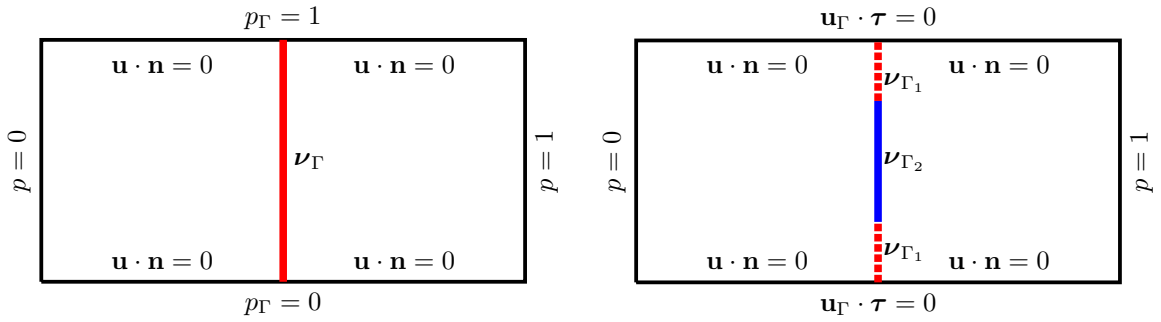

(a) Constant permeability

(b) Discontinuous permeability

Figure 4: Example 2: Computational domains and boundary conditions for the two test cases. In the second case, on the fracture, the permeable (red, dotted line) and impermeable (blue, solid line) areas are shown.

The obtained results are shown in Figure 5. For both cases (constant at the top, discontinuous at the bottom) we report the pressure field and Darcy velocity in the bulk (here the grid is very coarse only for visualization purposes) and the value of the pressure along the fracture. In the first case, since we have taken $\boldsymbol{\nu}_\Gamma^n = \boldsymbol{\nu}_\Gamma^\tau = 100 > 1$, we can observe that the fluid has the tendency to flow along the fracture. In the second case, one can see

that the part of the fracture with low (normal) permeability acts as a geological barrier, so that the fluid tends to avoid it and we can observe a jump of the bulk pressure across it. Our results are in agreement with those obtained in [62].

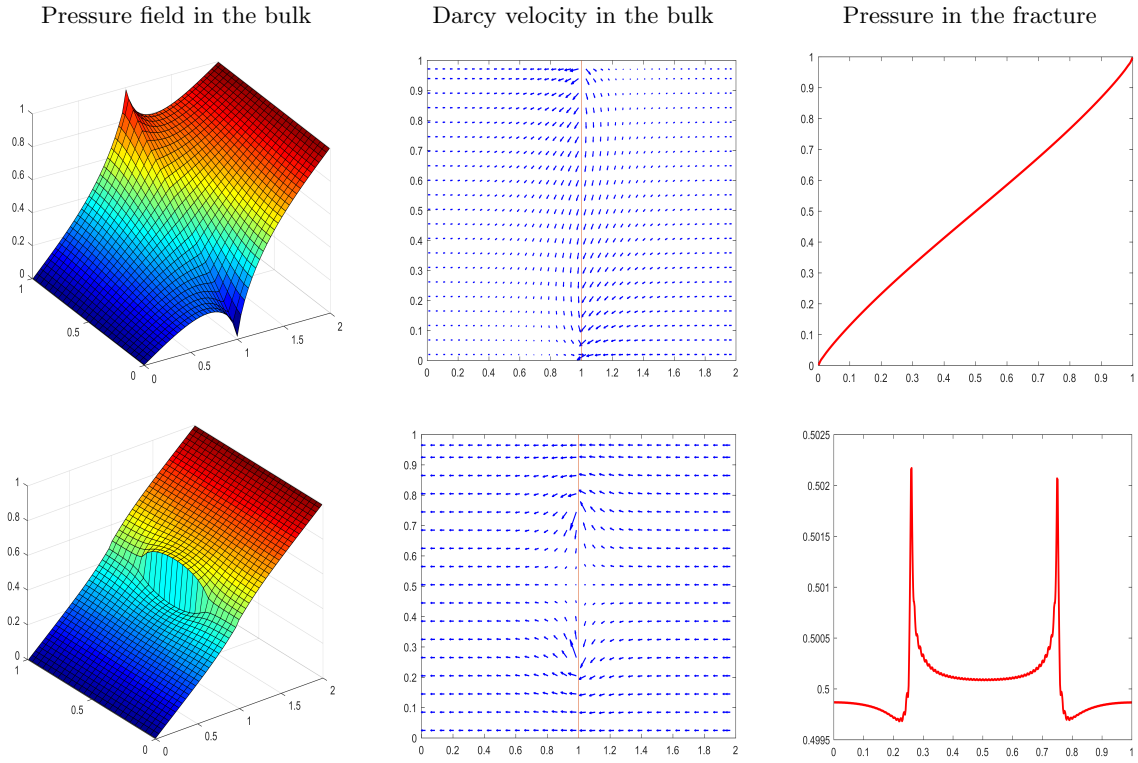

Figure 5: Example 2: Bulk pressure field (left), bulk Darcy velocity (middle) and fracture pressure (right) for the constant permeability (top) and discontinuous permeability (bottom) test cases.

6.3 Example 3: network of partially immersed fractures

With this last set of numerical experiments we investigate the capability of our discretization method to deal with more complicated geometrical configurations, considering a network of partially *immersed* fractures. Our reference is, in this case, [3], where the mathematical model developed in [62] has been extended to fully immersed fractures. In [9] we showed that our method in a *primal-primal* setting is capable of efficiently handling the configuration. Here, we reproduce the same numerical experiments to demonstrate that this holds true also in a *mixed-primal* setting.

In order to deal with immersed fractures, we need to supplement our model (6) with an equation describing the behaviour of the fracture pressure at the immersed tips. Following [3], we impose a homogeneous Neumann condition, thus assuming that the mass transfer across the immersed tips can be neglected, i.e., $\boldsymbol{\nu}_\Gamma^\tau \nabla_\tau p_\Gamma \cdot \boldsymbol{\tau} = 0$ on $\partial\Gamma$. At the extremities of the fractures that are non-immersed, i.e., $\partial\Gamma \cap \partial\Omega$, we impose boundary conditions that are consistent with those imposed on $\partial\Omega$ in that point.

We consider the bulk domain $\Omega = [0,1]^2$ cut by a network made of four partially immersed fractures: $\Gamma_1 = \{(x,y) \in [0,1]^2 : x \geq 0.3, y = 0.2\}$, $\Gamma_2 = \{(x,y) \in [0,1]^2 : x \leq 0.7, y = 0.4\}$,

$\Gamma_3 = \{(x, y) \in [0, 1]^2 : x \geq 0.3, y = 0.6\}$ and $\Gamma_4 = \{(x, y) \in [0, 1]^2 : x \leq 0.7, y = 0.8\}$. We perform two numerical experiments. In both of them, the fractures Γ_2 and Γ_4 are impermeable ($\boldsymbol{\nu}_\Gamma^\tau = \nu_\Gamma^n = 10^{-2}$), while Γ_1 and Γ_3 are partially permeable. In the first configuration, we consider for Γ_1 and Γ_3 the permeabilities $\nu_\Gamma^n = 10^{-2}$ and $\boldsymbol{\nu}_\Gamma^\tau = 100$, while in the second, we consider $\nu_\Gamma^n = 10^{-2}$ and $\boldsymbol{\nu}_\Gamma^\tau = 1$. Moreover, we vary the imposed boundary conditions as illustrated in Figure 6.

In both the experiments we consider an isotropic bulk permeability tensor i.e., $\boldsymbol{\nu} = \mathbf{I}$ and we assume that all the fractures have aperture $\ell_\Gamma = 0.01$. The flow is only generated by boundary conditions, since we take all the forcing terms $f = f_\Gamma = 0$. Finally, we choose as model parameter $\xi = 0.55$.

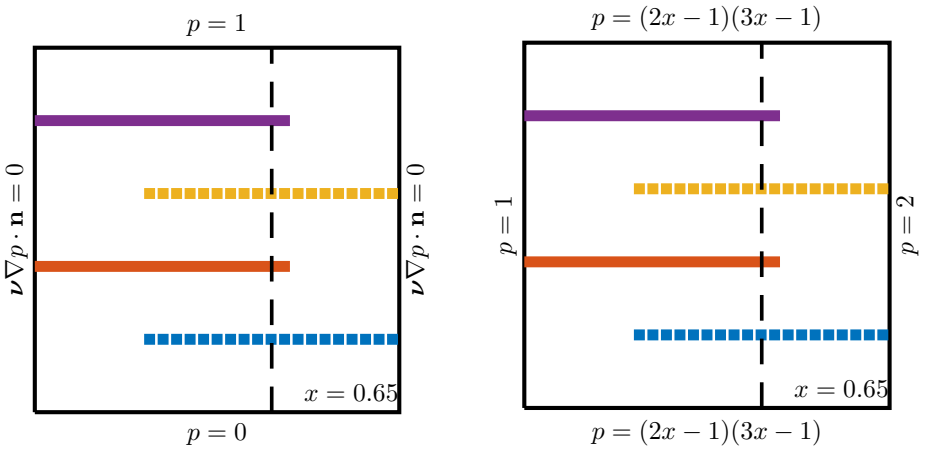

(a) Configuration 1: $\boldsymbol{\nu}_\Gamma^\tau = 100$ on Γ_1, Γ_3 (b) Configuration 2: $\boldsymbol{\nu}_\Gamma^\tau = 1$ on Γ_1, Γ_3

Figure 6: Example 3: Configurations and boundary condition for the two test cases.

To obtain our results, we employed cartesian grids featuring approximately the same number of elements as those employed in [3] and such that the immersed tips of the fractures coincide with one of the mesh vertices. For the approximation of the problem in the bulk and in the fracture we chose the polynomial degrees $k = k_\Gamma = 2$. In Figure 7, we show the results obtained for the two test cases with a mesh of 26051 elements. In particular, we report the pressure field in the bulk with the streamlines of the velocity (left), the value of the bulk pressure along the line $x = 0.65$ (middle) and the pressure field inside the four fractures (right). Our results are in perfect agreement with those obtained in [3] and in [9], thus showing that, also in a *mixed-primal* setting, our method is able to efficiently handle this configuration.

References

[1] C. Alboin, J. Jaffré, J. E. Roberts, and C. Serres. Modeling fractures as interfaces for flow and transport in porous media. In *Fluid flow and transport in porous media: mathematical and numerical treatment (South Hadley, MA, 2001)*, volume 295 of *Contemp. Math.*, pages 13–24. Amer. Math. Soc., Providence, RI, 2002.

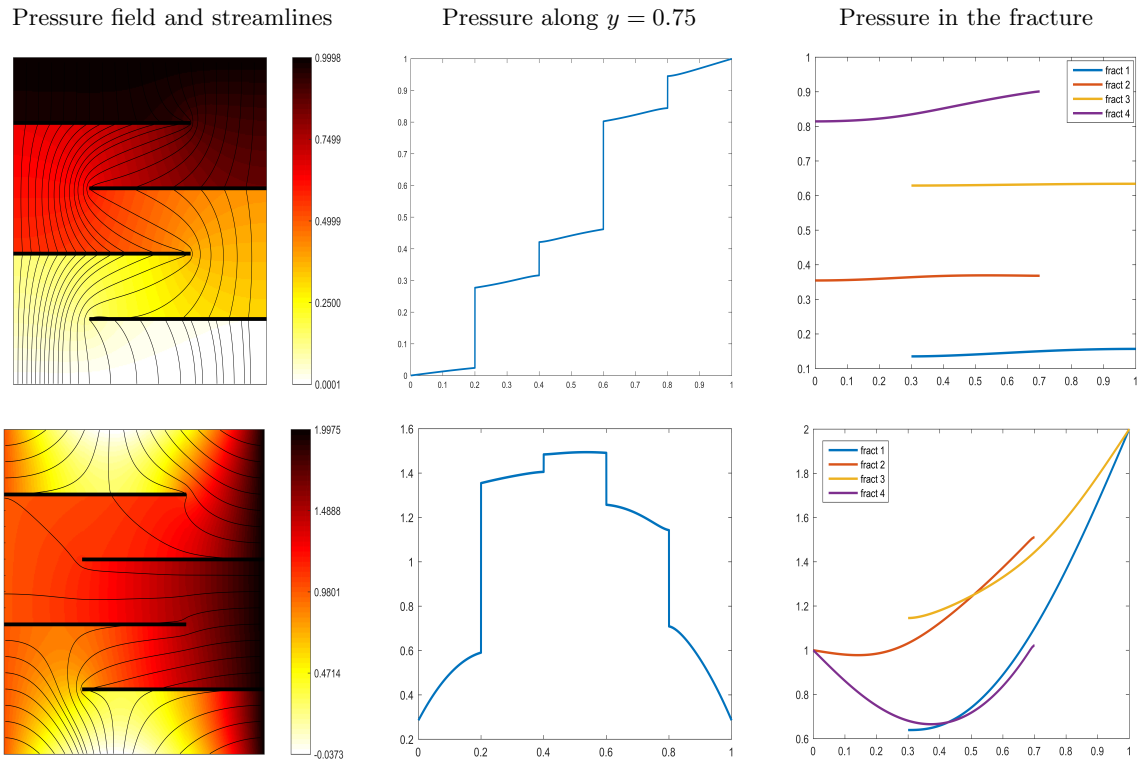

Figure 7: Example 3: first configuration (top) and second configuration (bottom).

[2] C. Alboin, J. Jaffré, J. E. Roberts, X. Wang, and C. Serres. Domain decomposition for some transmission problems in flow in porous media. In *Numerical treatment of multiphase flows in porous media*, volume 552 of *Lecture Notes in Phys.*, pages 22–34. Springer, Berlin, 2000.

[3] P. Angot, F. Boyer, and F. Hubert. Asymptotic and numerical modelling of flows in fractured porous media. *M2AN Math. Model. Numer. Anal.*, 43(2):239–275, 2009.

[4] P. F. Antonietti, F. Bonaldi, and I. Mazzieri. A high-order discontinuous Galerkin approach to the elasto-acoustic problem. *MOX report 18/2018. Submitted*, 2018.

[5] P. F. Antonietti, F. Brezzi, and L. D. Marini. Bubble stabilization of discontinuous Galerkin methods. *Comput. Methods Appl. Mech. Engrg.*, 198(21-26):1651–1659, 2009.

[6] P. F. Antonietti, A. Cangiani, J. Collis, Z. Dong, E. H. Georgoulis, S. Giani, and P. Houston. *Review of discontinuous Galerkin Finite Element Methods for partial differential equations on complicated domains*, volume 114 of *Lecture Notes in Computational Science and Engineering*, chapter 8, pages 281 – 310. Springer, 1st edition, 2016.

[7] P. F. Antonietti, L. B. da Veiga, D. Mora, and M. Verani. A stream Virtual Element formulation of the Stokes problem on polygonal meshes. *SIAM J. Numer. Anal.*, 52(1):386–404, 2014.

[8] P. F. Antonietti, L. B. da Veiga, S. Scacchi, and M. Verani. A C1 Virtual Element Method for the Cahn-Hilliard equation with polygonal meshes. *SIAM J. Numer. Anal.*, 54(1):34–56, 2016.

[9] P. F. Antonietti, C. Facciolà, A. Russo, and M. Verani. Discontinuous Galerkin Approximation of Flows in Fractured Porous Media on Polytopic Grids. *SIAM J. Sci. Comput.*, 41(1):A109–A138, 2019.

[10] P. F. Antonietti, L. Formaggia, A. Scotti, M. Verani, and N. Verzotti. Mimetic Finite Difference approximation of flows in fractured porous media. *ESAIM Math. Model. Numer. Anal.*, 50(3):809–832, 2016.

[11] P. F. Antonietti, S. Giani, and P. Houston. *hp*-version Composite Discontinuous Galerkin methods for elliptic problems on complicated domains. *SIAM J. Sci. Comput.*, 35(3):A1417–A1439, 2013.

[12] P. F. Antonietti, S. Giani, and P. Houston. Domain decomposition preconditioners for discontinuous Galerkin methods for elliptic problems on complicated domains. *J. Sci. Comput.*, 60(1):203–227, 2014.

[13] P. F. Antonietti and P. Houston. A class of domain decomposition preconditioners for *hp*-discontinuous Galerkin finite element methods. *Journal of Scientific Computing*, 46(1):124–149, 2011.

[14] P. F. Antonietti, P. Houston, X. Hu, M. Sarti, and M. Verani. Multigrid algorithms for *hp*-version interior penaty discontinuous Galerkin methods on polygonal and polyhedral meshes. *Calcolo*, 54(4):1169 – 1198, 2017.

[15] P. F. Antonietti, P. Houston, and G. Pennesi. Fast numerical integration on polytopic meshes with applications to discontinuous Galerkin finite element methods. *J. Sci. Comput.*, 77:1339–1370, 2018.

[16] P. F. Antonietti, G. Manzini, and M. Verani. The fully nonconforming Virtual Element Method for biharmonic problems. *Math. Mod. Meth. Appl. Sci.*, 28(02):387–407, 2018.

[17] P. F. Antonietti and I. Mazzieri. High-order Discontinuous Galerkin methods for the elastodynamics equation on polygonal and polyhedral meshes. *Computer Methods in Applied Mechanics and Engineering*, 342:414–437, 2018.

[18] P. F. Antonietti and G. Pennesi. V-cycle multigrid algorithms for discontinuous Galerkin methods on non-nested polytopic meshes. *Journal of Scientific Computing*, 78(1):625–652, 2019.

[19] D. N. Arnold. An interior penalty finite element method with discontinuous elements. *SIAM J. Numer. Anal.*, 19(4):742–760, 1982.

[20] D. N. Arnold, F. Brezzi, B. Cockburn, and L. D. Marini. Unified analysis of discontinuous Galerkin methods for elliptic problems. *SIAM J. Numer. Anal.*, 39(5):1749–1779, 2001/02.

[21] B. Ayuso de Dios, K. Lipnikov, and G. Manzini. The nonconforming Virtual Element Method. *ESAIM Math. Model. Numer. Anal.*, 50(3):879 – 904, 2016.

[22] F. Bassi, L. Botti, and A. Colombo. Agglomeration-based physical frame dG discretizations: an attempt to be mesh free. *Math. Mod. Meth. Appl. Sci.*, 24(8):1495–1539, 2014.

[23] F. Bassi, L. Botti, A. Colombo, D. A. Di Pietro, and P. Tesini. On the flexibility of agglomeration based physical space discontinuous Galerkin discretizations. *J. Comput. Phys.*, 231(1):45–65, 2012.

[24] F. Bassi, L. Botti, A. Colombo, and S. Rebay. Agglomeration based discontinuous Galerkin discretization of the Euler and Navier-Stokes equations. *Comput. & Fluids*, 61:77–85, 2012.

[25] L. Beirão da Veiga, F. Brezzi, A. Cangiani, G. Manzini, L. D. Marini, and A. Russo. Basic principles of Virtual Element Methods. *Math. Models Methods Appl. Sci.*, 23(1):199 – 214, 2013.

[26] L. Beirão da Veiga, F. Brezzi, L. D. Marini, and A. Russo. Mixed Virtual Element Methods for general second order elliptic problems on polygonal meshes. *ESAIM Math. Model. Numer. Anal.*, 50(3):727 – 747, 2016.

[27] L. Beirão da Veiga, F. Brezzi, L. D. Marini, and A. Russo. Virtual Element Method for general second-order elliptic problems on polygonal meshes. *Math. Models Methods Appl. Sci.*, 26(4):729 – 750, 2016.

[28] L. Beirão da Veiga, K. Lipnikov, and G. Manzini. *The Mimetic Finite Difference method for elliptic problems*, volume 11. Springer, Cham, 2014.

[29] M. F. Benedetto, S. Berrone, S. Pieraccini, and S. Scialò. The Virtual Element Method for discrete fracture network simulations. *Computer Methods in Applied Mechanics and Engineering*, 280:135–156, 2014.

[30] M. F. Benedetto, S. Berrone, and S. Scialò. A globally conforming method for solving flow in discrete fracture networks using the Virtual Element Method. *Finite Elements in Analysis and Design*, 109:23–36, 2016.

[31] F. Brezzi, K. Lipnikov, and M. Shashkov. Convergence of the Mimetic Finite Difference method for diffusion problems on polyhedral meshes. *SIAM J. Numer. Anal.*, 43(5):1872–1896 (electronic), 2005.

[32] F. Brezzi, K. Lipnikov, and M. Shashkov. Convergence of Mimetic Finite Difference method for diffusion problems on polyhedral meshes with curved faces. *Math. Mod. Meth. Appl. Sci.*, 16(2):275–297, 2006.

[33] F. Brezzi, K. Lipnikov, and V. Simoncini. A family of Mimetic Finite Difference methods on polygonal and polyhedral meshes. *Math. Mod. Meth. Appl. S.*, 15(10):1533–1551, 2005.

[34] E. Burman, P. Hansbo, M. G. Larson, and K. Larsson. Cut finite elements for convection in fractured domains. *Comput Fluids*, page in press, 2018.

[35] A. Cangiani, Z. Dong, and E. H. Georgoulis. *hp*-version space-time discontinuous Galerkin methods for parabolic problems on prismatic meshes. *SIAM J. Sci. Comput.*, 39(4):A1251–A1279, 2017.

[36] A. Cangiani, Z. Dong, E. H. Georgoulis, and P. Houston. *hp*-version discontinuous Galerkin methods for advection-diffusion-reaction problems on polytopic meshes. *ESAIM Math. Model. Numer. Anal.*, 50(3):699–725, 2016.

[37] A. Cangiani, Z. Dong, E. H. Georgoulis, and P. Houston. *hp-Version discontinuous Galerkin methods on polygonal and polyhedral meshes*. SpringerBriefs in Mathematics. Springer International Publishing, 2017.

[38] A. Cangiani, E. H. Georgoulis, and P. Houston. *hp*-version discontinuous Galerkin methods on polygonal and polyhedral meshes. *Math. Models Methods Appl. Sci.*, 24(10):2009–2041, 2014.

[39] A. Cangiani, G. Manzini, and O. J. Sutton. Conforming and nonconforming Virtual Element Methods for elliptic problems. *IMA J. Numer. Anal.*, 37(3):1317–1354, 2017.

[40] P. Castillo, B. Cockburn, I. Perugia, and D. Schötzau. An a priori error analysis of the local discontinuous Galerkin method for elliptic problems. *SIAM J. Numer. Anal.*, 38(5):1676–1706, 2000.

[41] F. A. Chave, D. Di Pietro, and L. Formaggia. A Hybrid High-Order method for Darcy flows in fractured porous media. *SIAM J. Sci. Comput.*, 40(2):A1063–A1094, 2018.

[42] B. Cockburn, B. Dond, and J. Guzmán. A superconvergent LDG-hybridizable Galerkin method for second-order elliptic problems. *Math. Comp.*, 77(264):1887–1916, 2008.

[43] B. Cockburn, J. Gopalakrishnan, and R. Lazarov. Unified hybridization of discontinuous Galerkin, mixed, and continuous Galerkin methods for second order elliptic problems. *SIAM J. Numer. Anal.*, 47(2):1319–1365, 2009.

[44] B. Cockburn, J. Gopalakrishnan, and F.-J. Sayas. A projection-based error analysis of HDG methods. *Math. Comp.*, 79(271):1351–1367, 2010.

[45] B. Cockburn, J. Guzmán, and H. Wang. Superconvergent discontinuous Galerkin methods for second-order elliptic problems. *Math. Comp.*, 78(265):1–24, 2009.

[46] B. Cockburn and C.-W. Shu. The local discontinuous Galerkin method for time-dependent convection-diffusion systems. *SIAM J. Numer. Anal.*, 35(6):2440–2463, 1998.

[47] C. D'Angelo and A. Scotti. A mixed finite element method for darcy flow in fractured porous media with non-matching grids. *ESAIM Math. Model. Numer. Anal.*, 46(02):465–489, 2012.

[48] D. A. Di Pietro and A. Ern. A Hybrid High-Order locking-free method for linear elasticity on general meshes. *Comput. Methods Appl. Mech. Engrg.*, 283(1):1–21, 2015.

[49] D. A. Di Pietro and A. Ern. Hybrid High-Order methods for variable-diffusion problems on general meshes. *C. R. Math. Acad. Sci. Soc. R. Can.*, 353(1):31–34, 2015.

[50] D. A. Di Pietro, A. Ern, and S. Lemaire. An arbitrary-order and compact-stencil discretization of diffusion on general meshes based on local reconstruction operators. *Comput. Method Appl. Math.*, 14(4):461–472, 2014.

[51] D. A. Di Pietro, A. Ern, and S. Lemaire. A review of hybrid high-order methods: formulations, computational aspects, comparison with other methods. In G. R. Barrenechea, F. Brezzi, A. Cangiani, and E. H. Georgoulis, editors, *Building bridges: connections and challenges in modern approaches to numerical partial differential equations*, volume 114 of *Lecture Notes in Computational Science and Engineering*. Springer, Cham, 2016.

[52] J. Droniou, R. Eymard, and R. Herbin. Gradient schemes: generic tools for the numerical analysis of diffusion equations. *ESAIM Math. Model. Numer. Anal.*, 50(3):749–781, 2016.

[53] B. Flemisch, A. Fumagalli, and A. Scotti. A review of the XFEM-based approximation of flow in fractured porous media. In *Advances in Discretization Methods*, pages 47–76. Springer, 2016.

[54] L. Formaggia, A. Scotti, and F. Sottocasa. Analysis of a mimetic finite difference approximation of flows in fractured porous media. *ESAIM Math. Model. Numer. Anal.*, 52(2):595–630, 2018.

[55] T.-P. Fries and T. Belytschko. The extended/generalized finite element method: an overview of the method and its applications. *Internat. J. Numer. Methods Engrg.*, 84(3):253–304, 2010.

[56] N. Frih, J. E. Roberts, and A. Saada. Modeling fractures as interfaces: a model for Forchheimer fractures. *Comput. Geosci.*, 12(1):91–104, 2008.

[57] A. Fumagalli and A. Scotti. A numerical method for two-phase flow in fractured porous media with non-matching grids. *Adv. Water Resour.*, 62, Part C:454–464, 2013.

[58] W. Hackbusch and S. A. Sauter. Composite Finite Elements for problems containing small geometric details. Part II: Implementation and numerical results. *Comput. Visual Sci.*, 1(4):15–25, 1997.

[59] W. Hackbusch and S. A. Sauter. Composite Finite Elements for the approximation of PDEs on domains with complicated micro-structures. *Numer. Math.*, 75(4):447–472, 1997.

[60] J. Hyman, M. Shashkov, and S. Steinberg. The numerical solution of diffusion problems in strongly heterogeneous non-isotropic materials. *J. Comput. Phys.*, 132(1):130–148, 1997.

[61] J. Jaffrré, M. Mnejja, and J. Roberts. A discrete fracture model for two-phase flow with matrix-fracture interaction. *Procedia Comput. Sci.*, 4:967 –973, 2011.

[62] V. Martin, J. Jaffré, and J. E. Roberts. Modeling fractures and barriers as interfaces for flow in porous media. *SIAM J. Sci. Comput.*, 26(5):1667–1691, 2005.

[63] I. Perugia and D. Schötzau. An *hp*-analysis of the local discontinuous Galerkin method for diffusion problems. *J. Sci. Comput.*, 17(1):561–571, 2002.

[64] I. Perugia and D. Schötzau. The *hp*-local discontinuous Galerkin method for low-frequency time-harmonic Maxwell equations. *Math. Comp.*, 72(243):1179–1214, 2003.

[65] E. M. Stein. *Singular integrals and differentiability properties of functions*, volume 2. Princeton university press, 1970.

[66] G. Strang and G. J. Fix. *An analysis of the finite element method*, volume 212. Prentice-Hall Englewood Cliffs, NJ, 1973.

[67] N. Sukumar and A. Tabarraei. Conforming Polygonal Finite Elements. *Internat. J. Numer. Methods Engrg.*, 61(12):2045–2066, 2004.

[68] A. Tabarraei and N. Sukumar. Extended Finite Element Method on polygonal and quadtree meshes. *Comput. Methods Appl. Mech. Eng.*, 197(5):425–438, 2008.

[69] C. Talischi, G. H. Paulino, A. Pereira, and I. F. Menezes. Polymesher: a general-purpose mesh generator for polygonal elements written in matlab. *Structural and Multidisciplinary Optimization*, 45(3):309–328, 2012.

[70] M. F. Wheeler. An elliptic collocation-finite element method with interior penalties. *SIAM J. Numer. Anal.*, 15(1):152–161, 1978.

MOX Technical Reports, last issues

Dipartimento di Matematica
Politecnico di Milano, Via Bonardi 9 - 20133 Milano (Italy)

08/2019 Prouse, G.; Stella, S.; Vergara, C.; Engelberger, S.; Trunfio, R.; Canevascini, R.; Quarteroni, A
Computational analysis of turbulent haemodynamics in radiocephalic arteriovenous fistulas with different anastomotic angles

04/2019 Delpopolo Carciopolo, L.; Formaggia, L.; Scotti, A.; Hajibeygi, H.
Conservative multirate multiscale simulation of multiphase flow in heterogeneous porous media

05/2019 Gasperoni, F.; Ieva, F.; Paganoni, A.M.; Jackson, C.; Sharples, L.
Evaluating the effect of healthcare providers on the clinical path of Heart Failure patients through a novel semi-Markov multi-state model

06/2019 Pagani, S.; Manzoni, A.; Carlberg, K.
Statistical closure modeling for reduced-order models of stationary systems by the ROMES method

07/2019 Dal Santo, N.; Manzoni, A.
Hyper-reduced order models for parametrized unsteady Navier-Stokes equations on domains with variable shape

03/2019 Ratti, L.; Verani, M.
A posteriori error estimates for the monodomain model in cardiac electrophysiology

02/2019 Micheletti, S.; Perotto, S.; Soli, L.
Topology optimization driven by anisotropic mesh adaptation: towards a free-form design

01/2019 Regazzoni, F.; Dedè, L.; Quarteroni, A.
Machine learning for fast and reliable solution of time-dependent differential equations

66/2018 Riccobelli, D.; Agosti, A.; Ciarletta, P.
On the existence of elastic minimizers for initially stressed materials

65/2018 Boschi, T.; Chiaromonte, F.; Secchi, P.; Li, B.
Covariance based low-dimensional registration for function-on-function regression